

THE UNIVERSITY OF ALBERTA

PHASE BEHAVIOR IN THE  
METHANE-CARBON DIOXIDE-ETHANE-N-HEXANE SYSTEM

BY



RONALD DAVID FRIESEN

A THESIS

SUBMITTED TO THE FACULTY OF GRADUATE STUDIES AND RESEARCH  
IN PARTIAL FULFILMENT OF THE REQUIREMENTS FOR THE DEGREE  
OF MASTER OF SCIENCE

DEPARTMENT OF CHEMICAL AND PETROLEUM ENGINEERING

EDMONTON, ALBERTA

FALL, 1972

## ABSTRACT

A high pressure apparatus for the study of vapor-liquid equilibrium in multicomponent systems has been developed. The mixture to be studied was contained between two pistons which were connected hydraulically to a double-acting Ruska pump. This allowed changing the system pressure without disturbing composition and also allowed the pistons to be moved up and down simultaneously while maintaining the volume between them constant. The cell contents were brought to equilibrium by circulating vapor externally and allowing it to bubble up through the liquid. Circulation was facilitated through the use of an externally mounted magnetic pump. Special valves allowed a small sample of either vapor or liquid to be isolated from the cell contents and analyzed by gas chromatography.

The equipment and experimental techniques were evaluated by obtaining vapor-liquid equilibrium data for the methane-normal hexane system at 77°F. A comparison with data from the literature showed agreement within 0.014 mole fraction for the liquid phase and 0.002 mole fraction for the vapor phase.

Vapor-liquid equilibrium data were obtained for two mixtures of the system methane-carbon dioxide-ethane-normal hexane above the critical temperature of each mixture. Retrograde behavior was observed. The experimental K-values were compared with predicted K-values obtained from the NGPSA data book, the BWR equation of state, the Chao-Seader correlation and the Chueh-Prausnitz correlation. Methane and ethane K-values were predicted fairly well by each method. The NGPSA data book and the BWR equation of state gave reasonable K-values for carbon dioxide. The predicted K-values of each of the four methods for normal hexane were

much lower than the experimental K-values. To properly evaluate the effect of carbon dioxide on the K-values of heavy components in multi-component hydrocarbon systems, more data are required.

TO MY WIFE

SHARON

## ACKNOWLEDGEMENTS

The author expresses his thanks to Dr. D. B. Robinson for his advice and understanding in the supervision of this project.

Special thanks are due to the personnel of the Chemical and Petroleum Engineering machine and instrument shops without whom the construction of the equipment would have been impossible.

To Dr. P. R. Bishnoi and Dr. G. R. J. Besserer for contributing their computer programs for the predictions of the data and for their good advise, the author expresses sincere thanks.

Also, thanks are due to Mr. J. Moser and Mr. J. Nagy for their assistance in establishing the computer monitored gas chromatograph system for this project.

Financial assistance from the Petroleum Recovery Research Institute is gratefully acknowledged.

TABLE OF CONTENTS

	<u>Page</u>
LIST OF TABLES	iii
LIST OF FIGURES	iv
I. INTRODUCTION	1
II. PREVIOUS RELATED WORK	6
III. EQUIPMENT DESIGN	9
A. Cell	9
B. Circulation System	12
C. Air Bath	12
D. Sampling Valves	13
IV. EXPERIMENTAL TECHNIQUES	15
A. Temperature Measurement	15
B. Pressure Measurement	15
C. Chromatographic Analysis	15
D. Materials	16
E. Preparation of Charge Gas	17
F. Charging the Cell	17
G. Sampling	18
V. EXPERIMENTAL RESULTS	19
VI. DISCUSSION OF RESULTS	25
A. Phase Behavior of the Methane-Normal Hexane System	25
B. Phase Behavior of the Methane-Carbon Dioxide-Ethane-Normal Hexane System	25
C. Comparison of Experimental Equilibrium Ratios with Predicted Values	26
(1) NGPSA Data Book	26
(2) BWR Equation of State	27

(3) Chao-Seader Correlation	28
(4) Chueh-Prausnitz Correlation	28
VII. CONCLUSIONS	31
REFERENCES	32
APPENDICES	
Appendix A Charging Procedure	34
Appendix B Sampling Procedure	35
Appendix C Tabulated Data	37
Appendix D Equipment Evaluation and Recommendations	54
Appendix E Calibrations	55
Appendix F Calculations	58

LIST OF TABLES

<u>Table No.</u>	<u>Title</u>	<u>Page</u>
1	Average Percent Deviations Between Experimental and Predicted K-values at 110°F	30
2	Average Percent Deviations Between Experimental and Predicted K-values at 140°F	30
3	Vapor-Liquid Equilibrium Data for the System Methane-Normal Hexane at 77°F	38
4	Comparison of Methane-Normal Hexane Liquid Phase Data with that of Shim and Kohn (18)	40
5	Comparison of Methane-Normal Hexane Vapor Phase Data with that of Shim and Kohn (18)	41
6	Experimental and Predicted Equilibrium Ratios for the Methane-Carbon Dioxide-Ethane-Normal Hexane System at 110°F	42
7	Experimental and Predicted Equilibrium Ratios for the Methane-Carbon Dioxide-Ethane-Normal Hexane System at 140°F	44
8	Percent Deviations Between Experimental and Predicted K-values at 110°F	46
9	Percent Deviations Between Experimental and Predicted K-values at 140°F	47
10	Vapor-Liquid Equilibrium Data for the Methane-Carbon Dioxide-Ethane-Normal Hexane System at 110°F	48
11	Vapor-Liquid Equilibrium Data for the Methane-Carbon Dioxide-Ethane-Normal Hexane System at 140°F	51



LIST OF FIGURES

<u>Figure No.</u>	<u>Title</u>	<u>Page</u>
1	Pressure-Temperature Diagram to Illustrate Retrograde Phenomena	2
2	Comparison of the Chao-Seader K-value Correlation with the Experimental Data of Yarborough and Vogel (3) to Illustrate the Failure of the Correlation Near the Convergence Pressure	5
3	Schematic Diagram of the Equilibrium Cell and its Associated Equipment	10
4	Essential Features of the Equilibrium Cell Design	11
5	Sampling Valve Schematic	14
6	Pressure-Composition Diagram for the System Methane-Normal Hexane at 77°F	20
7	Experimental K-values for the System Methane-Carbon Dioxide-Ethane-Normal Hexane at 110°F Compared to BWR and NGPSA Data Book Predictions	21
8	Experimental K-values for the System Methane-Carbon Dioxide-Ethane-Normal Hexane at 110°F Compared to Chueh-Prausnitz and Chao-Seader Predictions	22
9	Experimental K-values for the System Methane-Carbon Dioxide-Ethane-Normal Hexane at 140°F Compared to BWR and NGPSA Data Book Predictions	23
10	Experimental K-values for the System Methane-Carbon Dioxide-Ethane-Normal Hexane at 140°F Compared to Chueh-Prausnitz and Chao-Seader Predictions	24
11	Thermocouple Calibration	56
12	Transducer Calibration	57
13	Gas Chromatograph Temperature Enhancement Factor Curve	59

## I. INTRODUCTION

Physicists and chemists first began to study vapor-liquid equilibrium in the late nineteenth century. Initial work concentrated on pure components but soon expanded to include binary and multicomponent systems. The rapid expansion of the petroleum industry in the second quarter of the twentieth century produced a requirement for phase behavior data in hydrocarbon systems and in hydrocarbon systems containing non-hydrocarbon components.

A great deal of vapor-liquid equilibrium data has been accumulated over the years by a large number of investigators using a variety of experimental cells and methods. Many of the binary systems containing paraffin hydrocarbons have been investigated because of their usefulness in correlation development. Few multicomponent systems have been studied because of the difficulties encountered in studying systems containing three or more components as well as the fact that most attention has been given to binary systems. The problems of obtaining phase behavior data for multicomponent systems become even greater when conditions exist in which retrograde behavior occurs.

Retrograde phenomena were first described by Kuenen (1) in 1892. During compression of a binary mixture at a temperature above the critical temperature of the mixture, he observed the formation of a liquid at a certain pressure followed by vaporization of the liquid with further pressure increase. Katz and Kurata (2) describe retrograde behavior with the use of an assumed phase diagram such as that shown in Figure 1. Figure 1 is a simulated P-T diagram which might represent that of a complex mixture. The curve represented by KNITGC is the bubble point curve and the curve represented by LEMBC is the dew point curve.

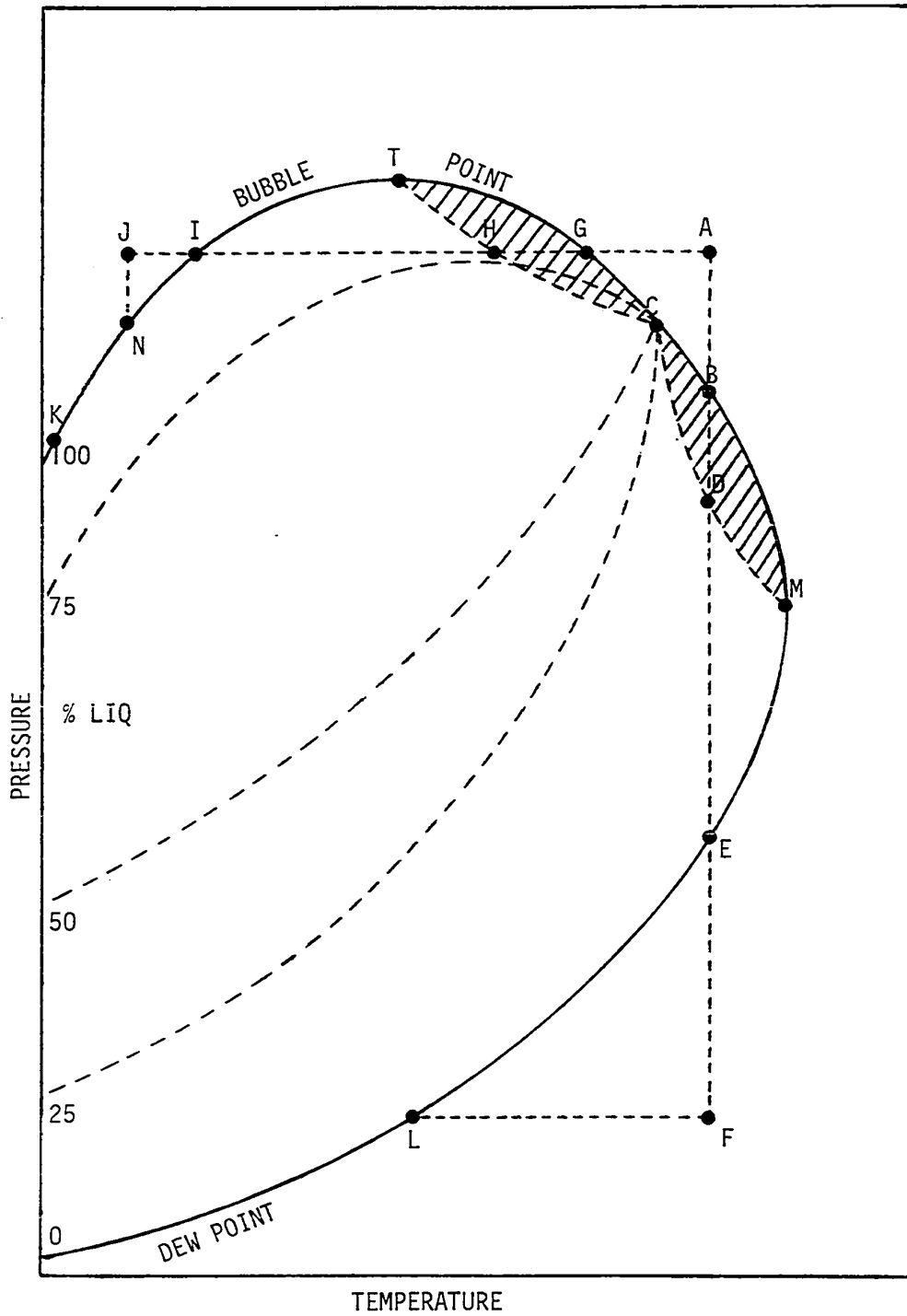


Figure 1 Pressure-Temperature Diagram to Illustrate Retrograde Phenomena

Point C represents the critical point of the mixture. The mixture at conditions corresponding to point A may be expanded at constant temperature to B at which pressure the first liquid will appear. Point B is called the upper dew point. Upon further isothermal expansion condensation continues until some point, D, is reached. Point D represents the conditions at which maximum liquid exists. Continued expansion at constant temperature from point D to point E results in vaporization of the liquid. Point E is called the lower dew point. The phenomenon observed between points B and D is known as retrograde condensation. Kuenen called this retrograde behavior of the "first kind". The fluid at conditions corresponding to A may be cooled at constant pressure to G at which temperature the first bubble of vapor will appear. Further isobaric cooling causes more vapor to form until some point, H, is reached. Point H represents the conditions at which maximum vapor exists. Constant pressure cooling from point H to point I results in normal condensation. The phenomena observed between points G and H is known as retrograde vaporization. Kuenen called this retrograde behavior of the "second kind". Moving in opposite directions results in opposite phenomena; for instance, from D to B is retrograde vaporization and from H to G is retrograde condensation. Point M is known as the cricondenthem temperature, the maximum temperature at which two phases can exist and point T is called the cricondenbar pressure, the maximum pressure at which two phases can exist. Isothermal retrograde phenomenon can occur only above the critical temperature, C, and below the cricondenthem temperature, M. Isobaric retrograde phenomenon can occur only above the critical pressure, C, and below the cricondenbar pressure, T. The only region in which retrograde phenomena can occur is that corresponding to the cross hatching in Figure 1.

Existing methods of predicting vapor-liquid equilibrium data fail in the critical region because the assumptions on which they are based do not apply in that region. The equations of state with which vapor phase fugacities are calculated can not cope with the high density vapors near the critical point. Solutions theories, used to obtain liquid phase fugacities, break down due to the rapid changes in density which take place near the critical point. Figure 2 shows the vapor-liquid equilibrium K-value data for ethane and normal decane in the system methane, ethane, propane, normal pentane, normal heptane, normal decane at 200°F obtained by Yarborough and Vogel (3). Plotted along with the experimental data are the corresponding K-values predicted by the Chao-Seader correlation. Figure 2 is presented to illustrate the typical behavior of the Chao-Seader correlation in the area near the convergence pressure of a mixture. Both the Chao-Seader and the Chueh-Prausnitz correlations exhibit this type of behavior. Thus, in order to predict vapor-liquid equilibrium K-values up to the convergence pressure of a mixture, a new approach is required. For proper development of a new approach, experimental data are required.

The primary objectives of this work may be stated as follows.

1. To develop a high pressure cell for obtaining vapor-liquid equilibrium data for multicomponent systems in regions near the critical point of the system.
2. To obtain vapor-liquid equilibrium data for the system methane, carbon dioxide, ethane, normal hexane at two temperatures greater than the critical temperature of the system.
3. To compare the experimental K-value data with K-values predicted by the NGLPSA data book, the BWR equation of state, the Chao-Seader correlation and the Chueh-Prausnitz correlation.

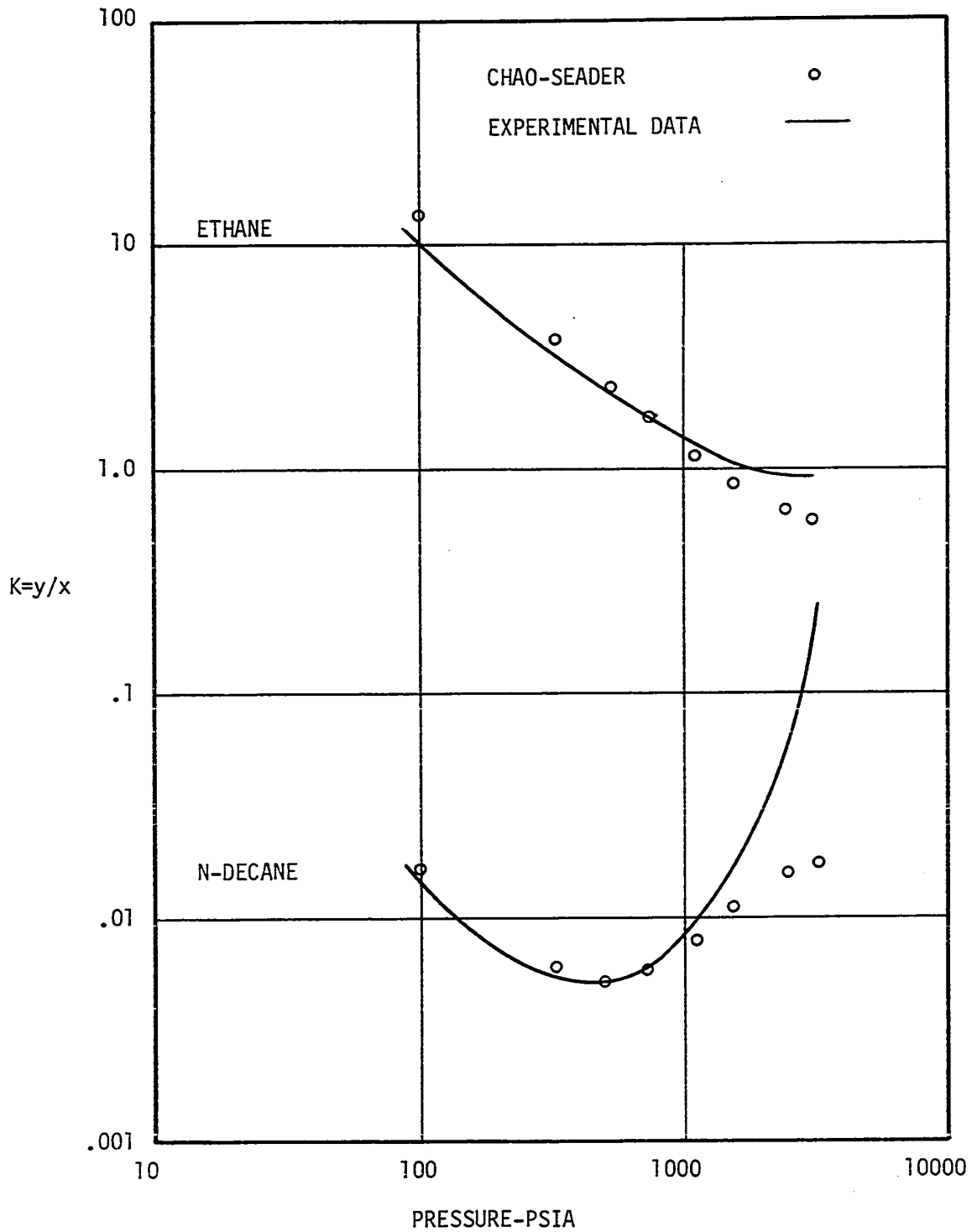


Figure 2 Comparison of the Chao-Seader K-value Correlation with the Experimental Data of Yarborough and Vogel (3) to Illustrate the Failure of the Correlation near the Convergence Pressure

## II. PREVIOUS RELATED WORK

Studies have been conducted on all six of the binary systems related to this work. Solid-liquid-vapor equilibrium data for the methane-carbon dioxide system in the temperature range from  $-100^{\circ}\text{F}$  to  $29^{\circ}\text{F}$  and for pressures as high as 1150 psia have been reported by Donnelly and Katz (4). Neumann and Walch (5) extended the data of Donnelly and Katz (4) down to  $-211^{\circ}\text{F}$ . Kaminishi, Arai, Saito and Maeda (6) obtained vapor-liquid equilibrium data for the methane-carbon dioxide system in the temperature range from  $-40^{\circ}\text{F}$  to  $14^{\circ}\text{F}$  and for pressures up to 1200 psia. Phase behavior data of the methane-carbon dioxide system along the solid-liquid-vapor locus from the triple point of carbon dioxide to  $-284^{\circ}\text{F}$  were reported by Davis, Rodewald and Kurata (7). Sterner (8) reported three phase data for the methane-carbon dioxide system in the region near the critical temperature of methane ( $-116^{\circ}\text{F}$ ).

Ruhemann (9) studied the phase behavior of the methane-ethane system at temperatures of  $-155^{\circ}\text{F}$  to  $32^{\circ}\text{F}$  and pressures up to 1250 psia. Ellington et al. (10) studied the methane-ethane system over the same range as Ruhemann (9) and found considerable disagreement of the two sets of data particularly in the critical region. Price and Kobayashi (11) and more recently Wichterle and Kobayashi (11a) reported vapor-liquid equilibrium data for the methane-ethane system at temperatures from  $-200^{\circ}\text{F}$  to  $50^{\circ}\text{F}$ . Their results were in good agreement with those of Ellington et al. (10).

The methane-normal hexane system has received considerable attention by several investigators. Frolich et al. (12) determined the solubility of methane in normal hexane at  $77^{\circ}\text{F}$  and at pressures up to 1300 psia. Hill and Lacey (13) measured the solubility of methane in normal hexane at  $86^{\circ}\text{F}$  and 300 psia. Sage, Webster and Lacey (14) made similar

Very little phase behavior data exist for systems in regions in which retrograde behavior occurs. Yarborough and Vogel (3) obtained K-values for a six-component normal paraffin mixture of methane, ethane, propane, normal pentane, normal heptane and normal decane at 200°F and over a pressure range from 100 to 3000 psia. Vairogs, Klekers and Edmister (24) studied two mixtures of the methane, ethane, propane, normal pentane, normal hexane, normal decane system at 150° and 250°F and at pressures ranging from 100 to 4000 psia. Gonzalez and Lee (25) obtained upper and lower dew points for several mixtures containing varying amounts of nitrogen, helium, methane, ethane, propane, normal butane, normal pentane, normal hexane and normal heptane.



measurements at temperatures between 100°F and 220°F and at pressures up to 2500 psia. Bubble and dew point densities and compositions at 25°, 55° and 85°C for pressures up to 230 atm were reported by Boomer and Johnson (15) for methane-normal hexane mixtures which contained small amounts of nitrogen. Schoch, Hoffmann and Mayfield (16) determined the solubilities of methane in normal hexane at 160°F and 220°F for pressures up to the critical. Stepanova and Vybornova (17) reported the critical pressure and equilibrium constants for the methane-normal hexane system between 50 and 210 atm and 0° and 60°C. Shim and Kohn (18) determined vapor-liquid equilibrium data for the methane-normal hexane system at temperatures between -110° and 150°C and pressures up to 160 atm. Poston and McKetta (19) obtained vapor-liquid equilibrium data for the methane-normal hexane system at temperatures between 100° and 340°F and pressures up to 2902 psia. Their work included data in the critical region which had been unattainable by previous authors.

The remaining binaries, carbon dioxide-ethane, carbon dioxide-normal hexane and ethane-normal hexane have not been investigated as thoroughly as the previous three. Khazanova et al. (20) obtained phase behavior data for the carbon dioxide-ethane system at temperatures from 10° to 20°C and at pressures up to 62 atm. The carbon dioxide-normal hexane system at temperatures between 100° and 300°F and at pressures up to 1700 psia was studied by Gupta (21). Some discrepancies in his data were corrected by Friesen and Robinson (22). Zais and Silberberg (23) determined vapor and liquid equilibrium phase compositions in the ethane-normal hexane system at 150°, 250° and 350°F and at pressures from 60 psia to near the critical.

### III. EQUIPMENT DESIGN

Figure 3 is a schematic representation of the apparatus and its accompanying equipment. The cell and circulation system are enclosed in an air bath shown in Figure 3 by dotted lines. Details of the major pieces of equipment will be dealt with in separate sections.

#### A. Cell

A high pressure vessel was required to obtain vapor-liquid equilibrium data for a multicomponent system in the retrograde region. To accomplish this, the volume of the vessel had to be large enough to obtain adequate liquid for sampling near the dew points. In addition the volume had to be variable to allow changes of pressure without affecting composition.

The main features of the cell are shown in Figure 4. All parts were machined of 316 stainless steel. The cell is 61.6 cm high and has a maximum working volume of 600 cc when assembled. It consists of three parts, the two end sections containing pistons and the middle section containing windows. The pistons serve to separate the cell contents from the driving fluid and facilitate volume changes. The piston seal is provided by three neoprene O-rings while two teflon guides keep the piston parallel to the cylinder walls. Technical grade mercury is used as the driving fluid. Horizontal section A-A shows the position of the two windows, the thermocouple, and one of the two circulation ports. The windows are pyrex glass disks 2.9 cm in diameter and 2.5 cm thick. Bolted cover plates hold the windows securely against lapped surfaces where 1.5 mm thick glass-filled teflon gaskets provide the seal. The thermocouple is made of iron-constantan sheathed in 316 stainless steel

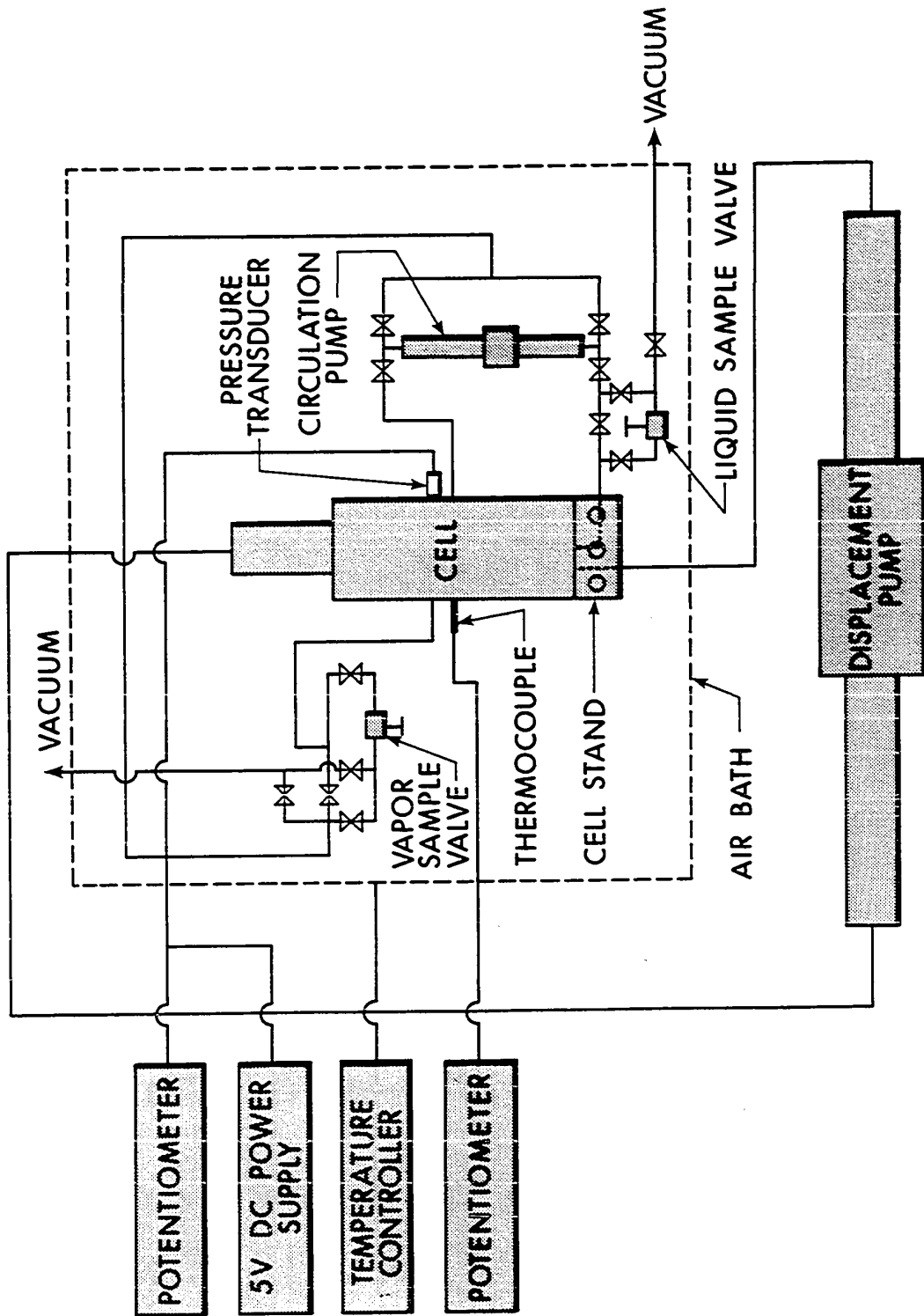
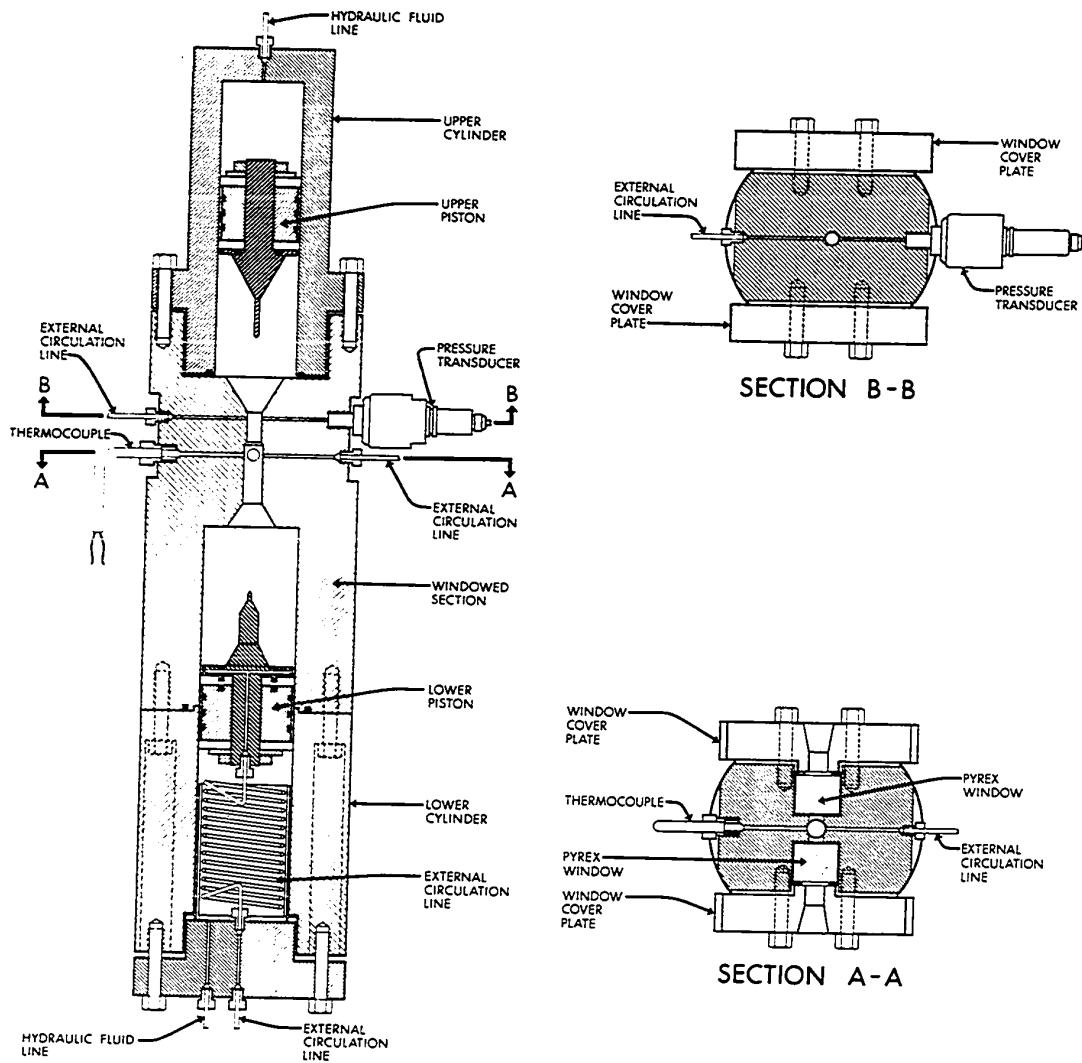


Figure 3 Schematic Diagram of the Equilibrium Cell and Its Associated Equipment



APPROX. SCALE: 1 INCH = 4 1/2 INCHES

Figure 4 Essential Features of the Equilibrium Cell Design

and has its tip exposed to the cell contents. Horizontal section B-B shows the position of the pressure transducer and the other circulation port. The pressure transducer is a Statham model UC3 with a 5000 psi diaphragm.

The lower piston assembly deserves more detailed description. The piston proper has a tube extending up the middle connected via six radial tubes to holes drilled through the piston face. The lower end of the tube is connected to a coil consisting of 1/8 in. thin wall stainless steel tubing. The coil expands and contracts, thus allowing the piston to move freely in the cylinder and providing an avenue through which vapor can be circulated to bubble through the liquid.

#### B. Circulation System

The cell contents are brought to equilibrium by circulating vapor from one of the ports through a magnetic pump back into the cell through the bottom piston where it bubbles through the liquid. Details of the circulation system are shown in Figure 3. The magnetic pump was machined according to a Ruska design and driven by a Graham variable speed transmission unit. Two ports through which vapor may be drawn are provided. The upper one is used in conjunction with the vapor sampling valve and the lower one for equilibrating. The total volume of the circulating system is 50 cc.

#### C. Air Bath

The cell and circulating system are maintained at a constant temperature by a temperature controlled air bath. The bath is a box framed with 3/8 in. plywood on the outside and lined with asbestos board on the inside. A two inch space between the plywood and asbestos

board is filled with fiberglas insulation. Visual observation of the cell is made possible through a double glass door which also provides access to the liquid sampling valve. Access to the vapor sampling valve is gained through another door. Two glove-and-sleeve arrangements make it possible to operate the valves in the circulation system. An electric air duct heater and a copper coil provide the heating and cooling. The air within the bath is circulated by a 12 in. fan. The temperature is controlled by an external Hallikainen Model 1253 Thermotrol with a Hallikainen Model 1085 resistance thermometer immersed in the bath. The temperature is controlled to within  $\pm 0.1^{\circ}\text{F}$ .

#### D. Sampling Valves

The sampling valves are of the type described by Yarborough and Vogel (3). The main modification was to drill the sample cavity into the stem of a stainless steel screw which was then fitted into the base of the valve. This made varying the sample size possible simply by interchanging screws with varying cavity sizes. A cavity size of 0.004 cc is used for liquid sampling. For vapor sampling at pressures less than 1000 psia a cavity size of 0.02 cc is used and at pressures greater than 1000 psia the cavity size is changed to 0.01 cc. Figure 5 shows the main features of the sampling valve.

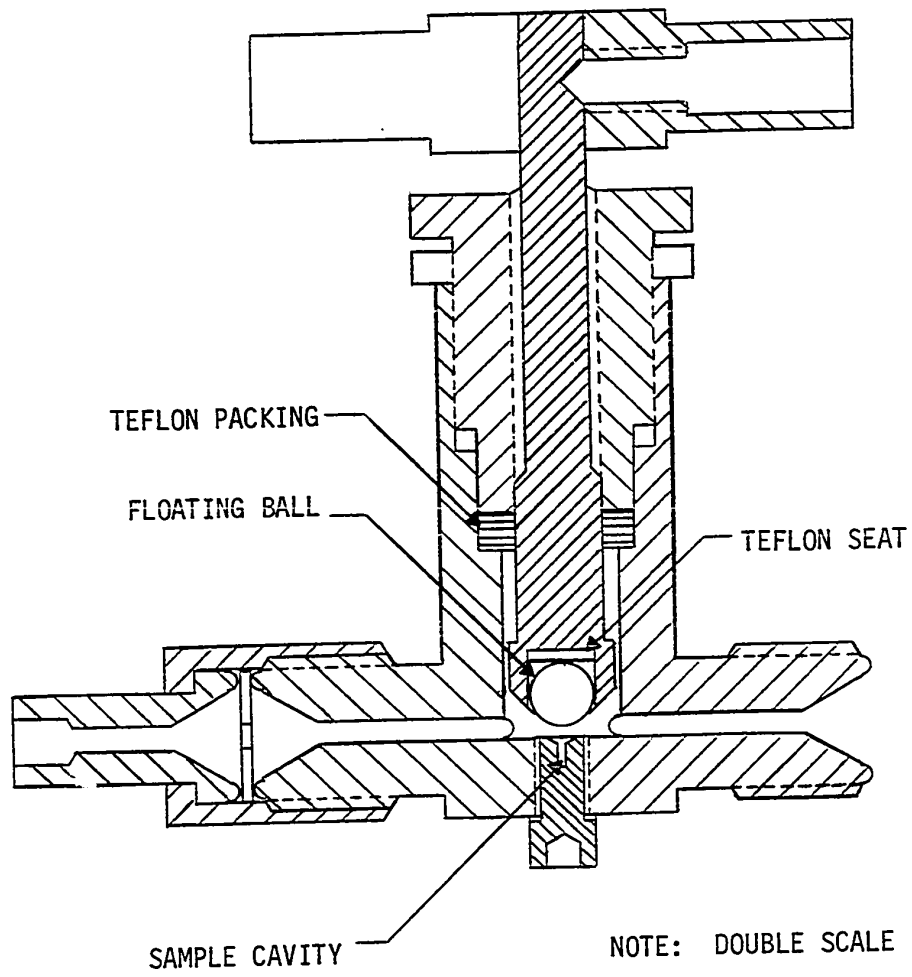


Figure 5 Sampling Valve Schematic

#### IV. EXPERIMENTAL TECHNIQUES

##### A. Temperature Measurement

The temperature of the cell contents was measured using an iron-constantan thermocouple and a Leeds and Northrup Model 8686 millivolt potentiometer. The thermocouple was calibrated to an accuracy of  $\pm 0.1^{\circ}\text{C}$ . The temperature was monitored continuously on a Hewlett-Packard Model 7100B recorder which allowed variations as small as  $0.1^{\circ}\text{C}$  to be detected. Figure 11 in Appendix E shows the calibration curve for the thermocouple.

##### B. Pressure Measurement

A Statham Model UC3 transducer with a 5000 psi diaphragm was used to measure the pressure of the cell contents. A Hewlett-Packard Model 6101A constant D.C. power supply provided the operational voltage to the transducer. The output from the transducer was read on a Leeds and Northrup Model 8686 millivolt potentiometer. The transducer was calibrated using the vapor pressure of carbon dioxide at known temperatures and is believed accurate to within  $\pm 3$  psia. The calibration was checked for linearity at higher and lower pressures than were attainable using the vapor pressure of carbon dioxide by connecting a Heise gauge into the system. Figure 12 of Appendix E shows the calibration curve for the transducer.

##### C. Chromatographic Analysis

Sample analysis was accomplished using a Hewlett-Packard Model 5750 gas chromatograph with matching Porapak Q columns. In order to shorten the time required for analysis it was necessary to program the column oven from room temperature to  $200^{\circ}\text{C}$ . Since column temperature



affects column response, a curve of column temperature versus enhancement factor was required. This curve was obtained by running samples of equal size through the column at varying temperatures and measuring the area of the peaks obtained. Figure 13 of Appendix F shows the resulting curve. The response factors of Messner, Rosie, and Argabright (26) for methane, carbon dioxide, ethane and normal hexane were used to calculate the mole fractions of these components. The factors were tested on known samples using the enhancement factors of Figure 13 and were found to give answers accurate to  $\pm 0.001$  mole fraction. The column conditions for the analysis of the methane-normal hexane mixture were:

Column	:	Porapak Q
Column Length	:	6 feet
Carrier Gas	:	Helium at 45 ml/min
Detector Current	:	150 ma
Column Temperature	:	200°C
Sample Size	:	0.004 ml to 0.02 ml

The column conditions for the analysis of the methane-carbon dioxide-ethane-normal hexane mixtures were:

Column	:	Porapak Q
Column Length	:	6 feet
Carrier Gas	:	Helium at 35 ml/min (average)
Detector Current	:	150 ma
Column Temperature	:	Room temperature to 200°C
Sample Size	:	0.004 ml to 0.02 ml

#### D. Materials

Matheson ultra high purity methane with a stated analysis of 99.97 mole percent methane was used. Carbon dioxide was obtained from Canada Liquid Air Limited. Analysis showed it to contain in excess of 99.9 mole percent carbon dioxide. Research grade ethane with a reported analysis of 99.94 mole percent ethane was obtained from Phillips Petroleum Company. Normal hexane was obtained from Fisher Scientific

the presence of only one phase was assured. This was in excess of 2500 psia. The contents were further circulated until homogeneity was achieved. When a sample taken from the bottom of the cell agreed with a sample taken from the top homogeneity was assumed. A more detail step by step charging procedure is given in Appendix A.

G. Sampling

Sampling was done by allowing a portion of the phase to be sampled to fill the cavity of the appropriate sampling valve, isolating the cavity from the system and then physically moving the sampling valve to the chromatographic loop for analysis. This was done by opening and closing the appropriate valves of the circulating system. A detailed step by step description of the sampling procedure is given in Appendix B.

Company and had a reported analysis of 99.0 mole percent normal hexane. Chromatographic analysis showed this to be considerably low. It was estimated that the analysis was at least 99.5 mole percent normal hexane with the remaining 0.5 mole percent being mainly hexane isomers.

E. Preparation of Charge Gas

Methane, ethane and carbon dioxide were mixed in a known proportion in a cylinder and the contents tested for homogeneity by chromatographic analysis at certain time intervals. Mixing was achieved by inducing convection currents in the cylinder through the use of a strip heater along one side of the cylinder. When sequential analyses were the same, homogeneity of mixture was assumed. The mixture in the cylinder had the following analysis:

<u>Component</u>	<u>Mole Fraction</u>
Methane	0.8289
Carbon Dioxide	0.0993
Ethane	0.0718

F. Charging the Cell

Before charging, the cell and circulation system were evacuated. Five cubic centimeters, representing approximately 0.0385 gram moles of normal hexane were then introduced into the cell. Based on a calculation of the volumetric behavior of the gas mixture, it was estimated that charge gas added to the cell and circulation system at a pressure of 220 psia would give the desired charge composition. After the addition of the components was completed the circulation system was put in operation for about three hours to allow thorough mixing of cell constants. Using the cell pistons, the mixture was compressed to a pressure at which

## V. EXPERIMENTAL RESULTS

Vapor-liquid equilibrium data were obtained for the methane-normal hexane system at 77°F. This served to test all equipment and to develop operational procedures. The raw data are tabulated in Table 3 of Appendix C. The smoothed data are shown in Figure 6 plotted on pressure-composition coordinates. Shown with the data of this work are those obtained by Shim and Kohn (18). Tables 4 and 5 of Appendix C present a comparison of the data of this work with those of Shim and Kohn (18) in the vapor and liquid phases respectively. A maximum difference of 0.002 mole fraction in the vapor phase and 0.014 mole fraction in the liquid phase exists between the data of Shim and Kohn (18) and the data of the present work.

Data were obtained at two temperatures for the methane-carbon dioxide-ethane-normal hexane system. The data obtained at 110°F are tabulated in Table 10 of Appendix C and the data obtained at 140°F are tabulated in Table 11 of Appendix C. The equilibrium ratios for each component were calculated and smoothed. The smooth equilibrium ratios are shown in Figures 7 to 10 plotted against pressure on log-linear coordinates. Plotted with the experimental equilibrium ratios are predicted K-values obtained from the following correlations: Chao-Seader (36, 37, 38, 39), Chueh-Prausnitz (34), BWR equation of state using the Bishnoi-Robinson (29, 30, 31) mixing rules and NGPSA data book (27). The smoothed experimental K-values along with the K-values predicted by each correlation are tabulated in Tables 6 and 7 for the 110°F and 140°F isotherms respectively.

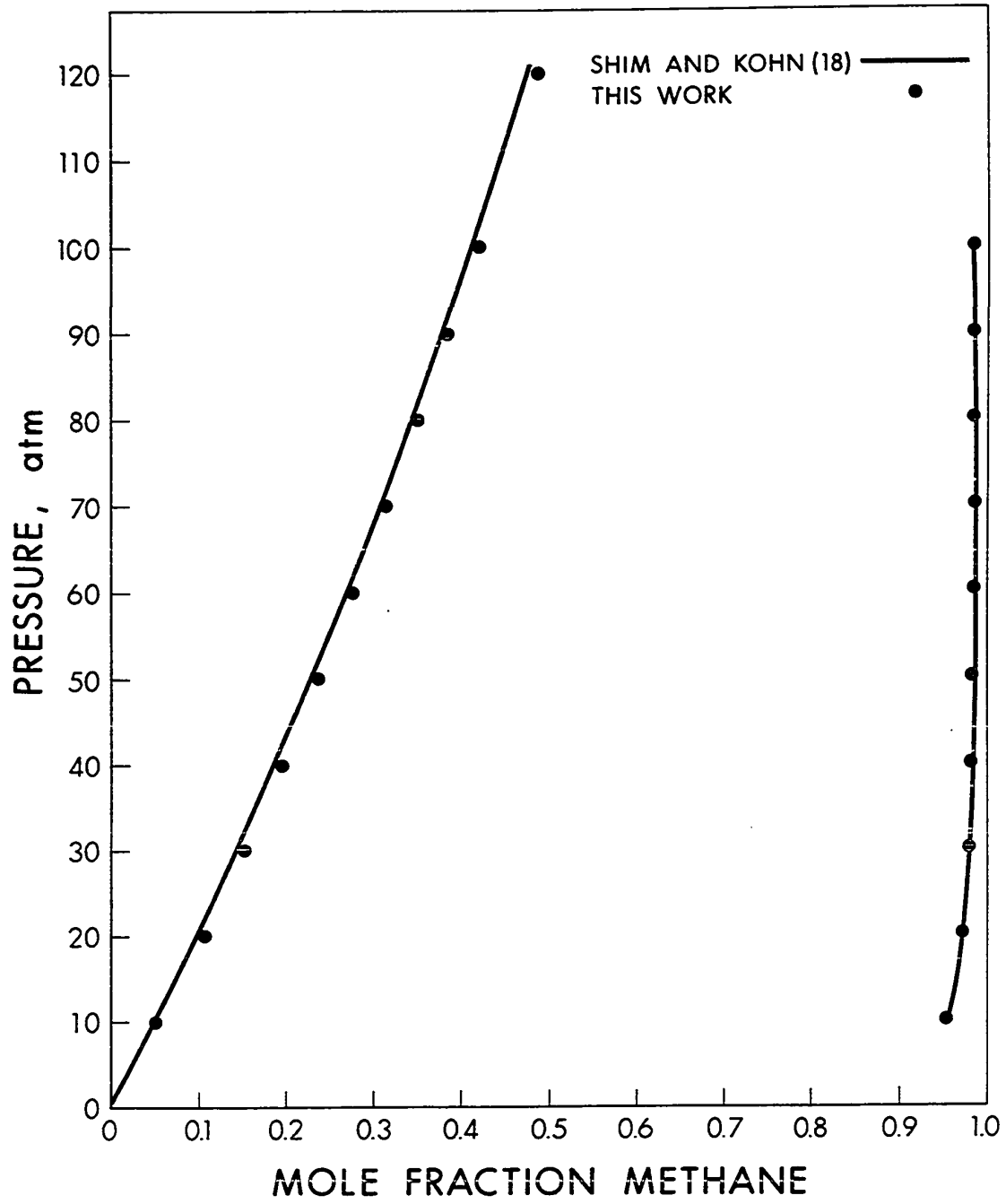


Figure 6 Pressure-Composition diagram for the System Methane-Normal Hexane at 77°F

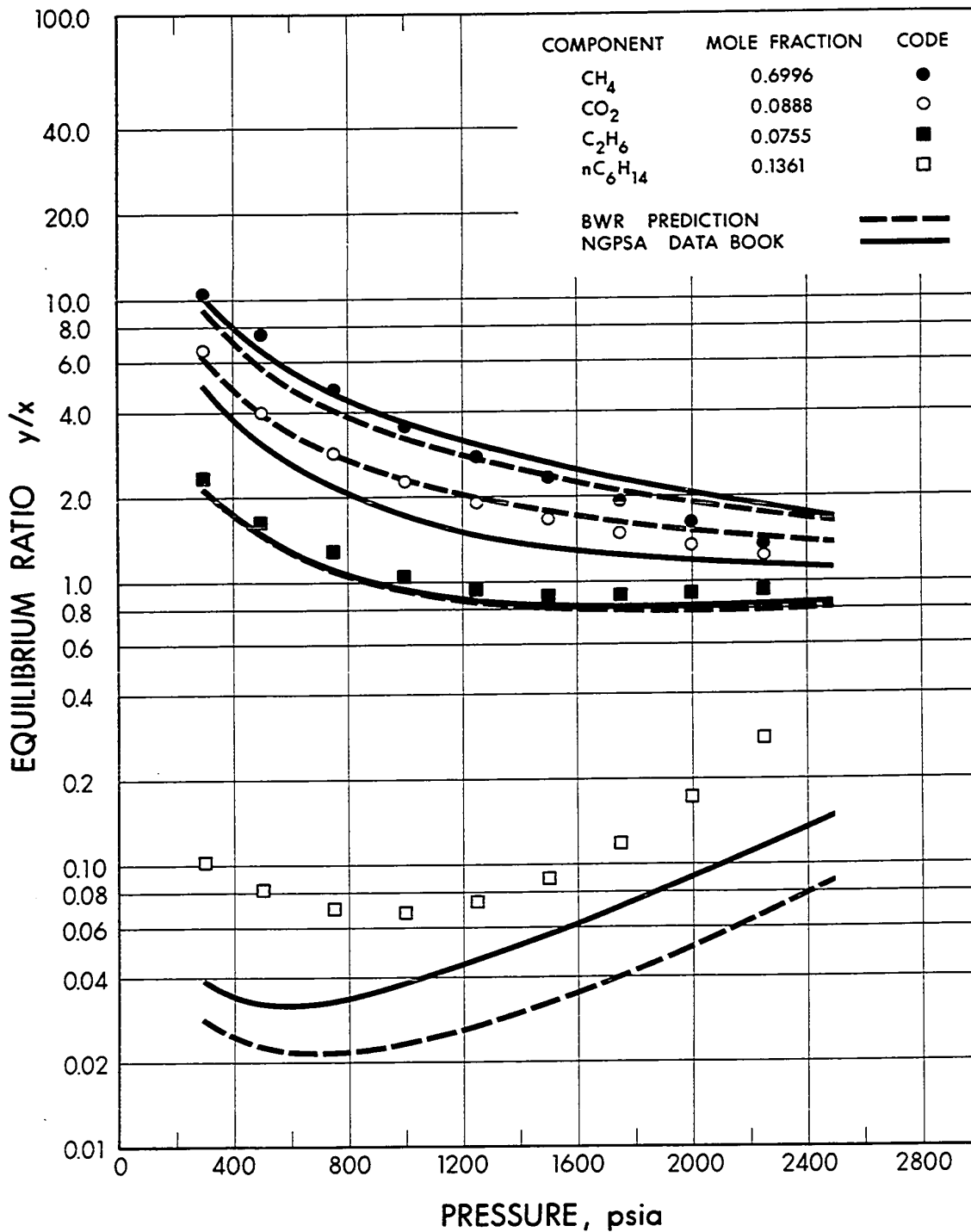


Figure 7 Smoothed Experimental K-values for the System Methane-Carbon Dioxide-Ethane-Normal Hexane at 110°F Compared to BWR and NGPSA Data Book Predictions

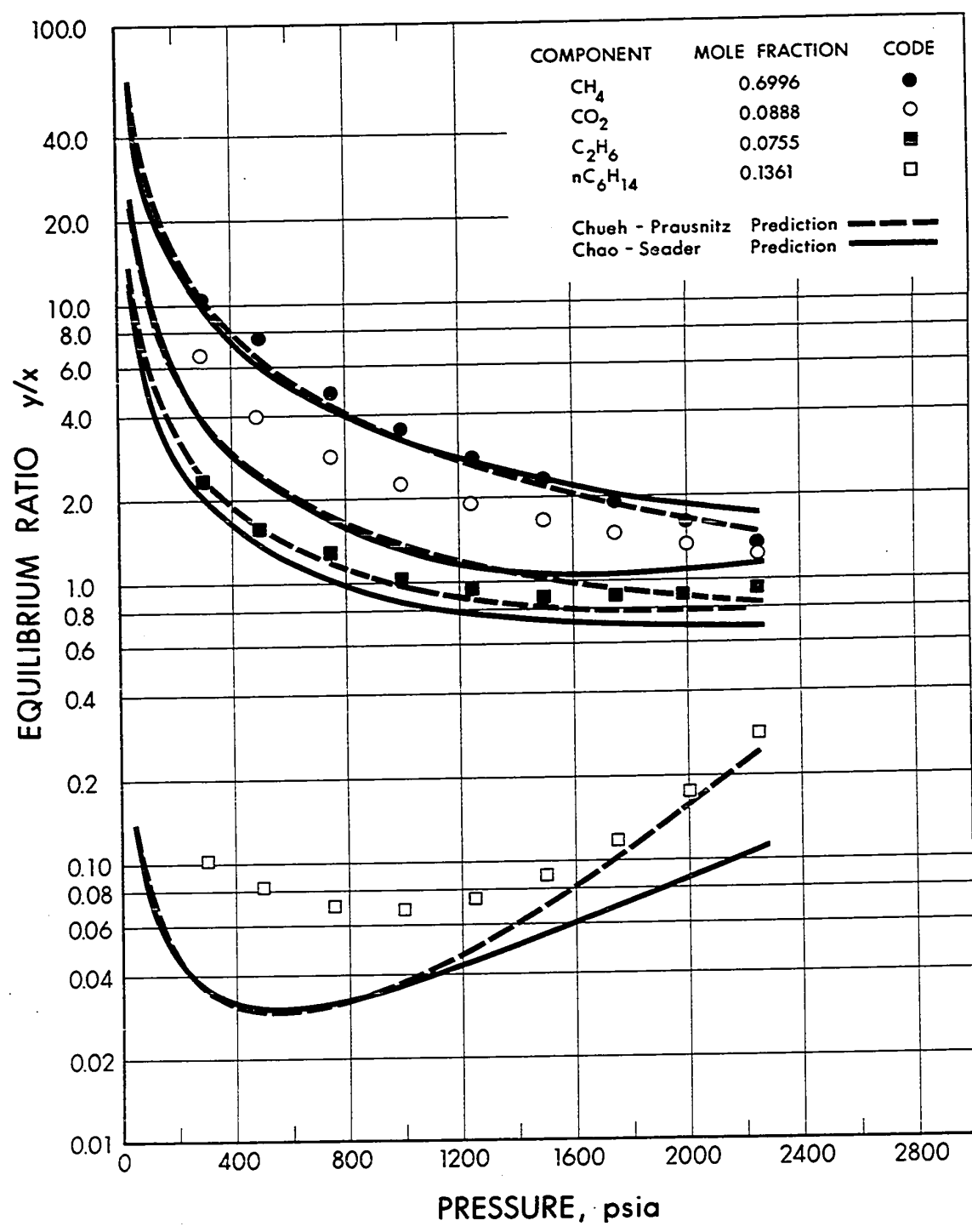


Figure 8 Smoothed Experimental K-values for the System Methane-Carbon Dioxide-Ethane-Normal Hexane at 110°F Compared to Chueh-Prausnitz and Chao-Seader Predictions

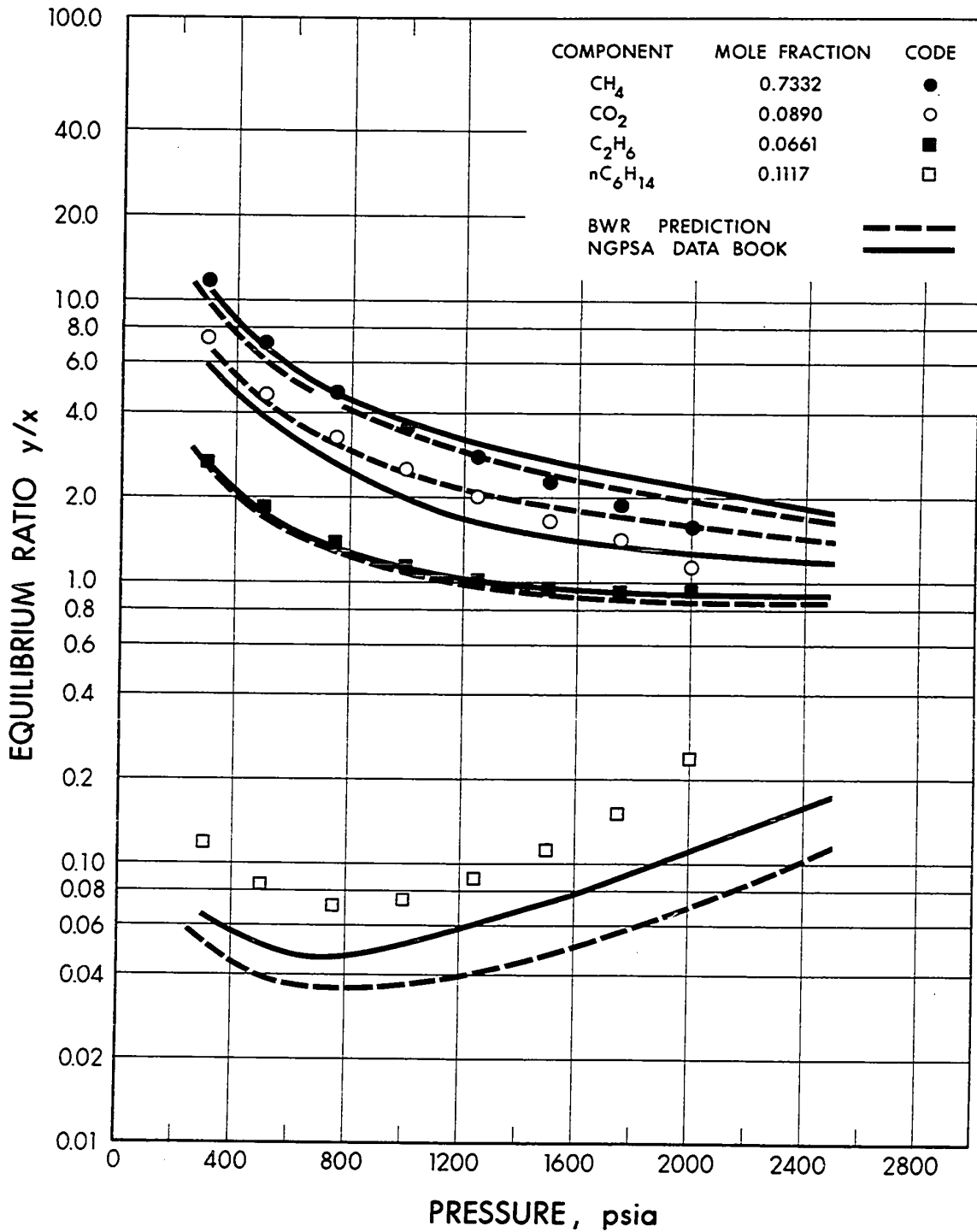


Figure 9 Smoothed Experimental K-values for the System Methane-Carbon Dioxide-Ethane-Normal Hexane at 140°F Compared to BWR and NGPSA Data Book Predictions



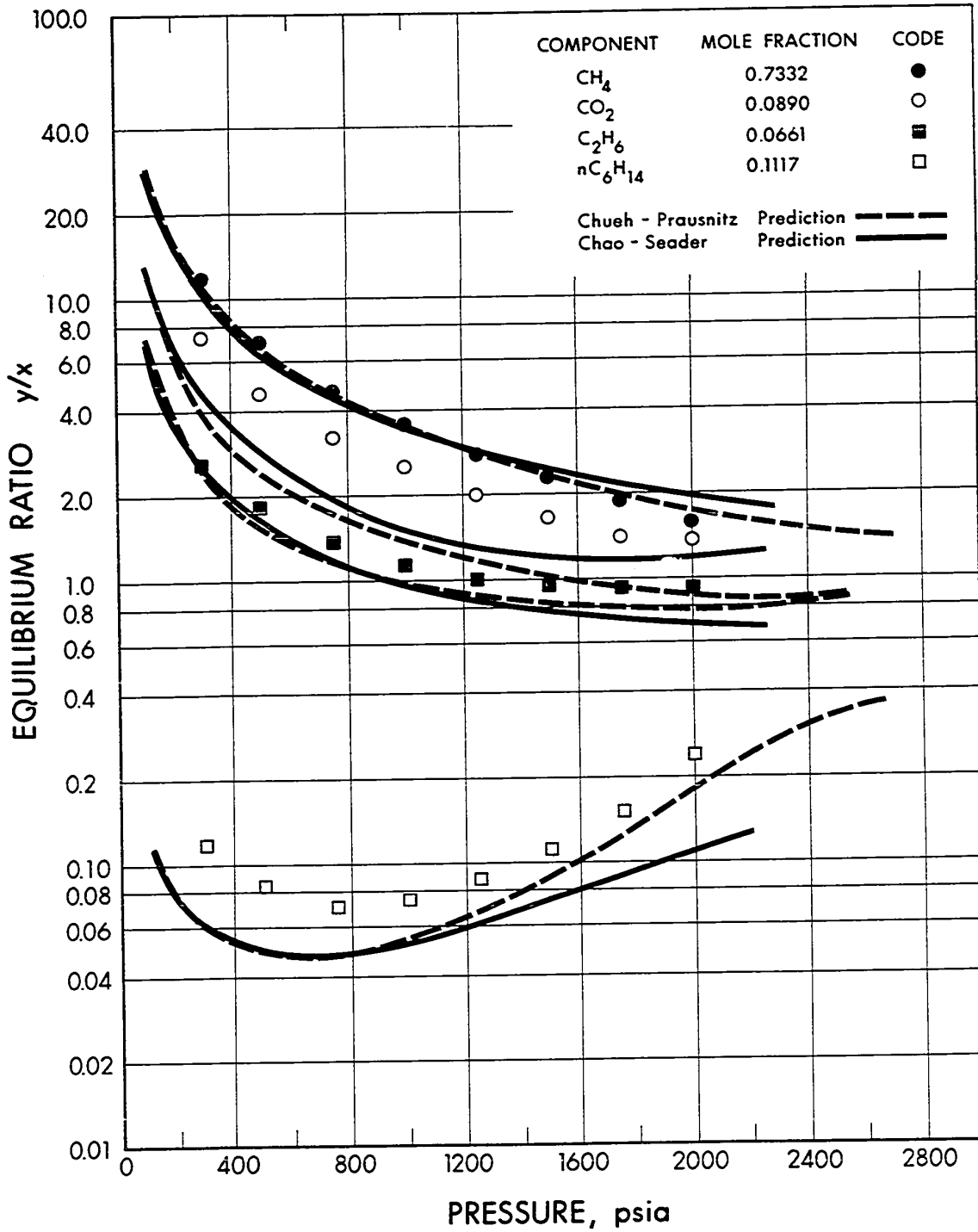


Figure 10 Smoothed Experimental K-values for the System Methane-Carbon Dioxide-Ethane-Normal Hexane at 140°F Compared to Chueh-Prusnitz and Chao-Seader Predictions

## VI. DISCUSSION OF RESULTS

### A. Phase Behavior of the Methane-Normal Hexane System

The vapor-liquid equilibrium data for the system methane-normal hexane obtained in this study are in good agreement with the data reported by Shim and Kohn (18) as shown in Figure 6. In the liquid phase the differences between the values obtained in this work and the data of Shim and Kohn are all positive and are less than 0.01 mole fraction in all cases except for the point at 120 atm, the average difference being 0.0074 mole fraction. Table 4 of Appendix C gives the difference between the value of this work and that of Shim and Kohn at each point in the liquid phase. Table 5 of Appendix C gives a similar comparison for the vapor phase. In the vapor phase both negative and positive differences occur, the absolute average difference being 0.0009 mole fraction. The results showed that the experimental techniques were good and that the equipment was in working order.

### B. Phase Behavior of the Methane-Carbon Dioxide-Ethane-Normal Hexane System

The mixtures of methane-carbon dioxide-ethane and normal hexane were chosen in such a way that vapor-liquid equilibrium data could be obtained in the two phase region above the critical temperature. Both mixtures studied exhibited retrograde behavior, but because it was impossible to measure the percent liquid in the cell, the exact pressure at which retrograde behavior began was not obtained. However an estimate of this pressure was made and is thought to be accurate to within  $\pm 50$  psia. The isotherm at 140°F began to exhibit retrograde behavior at about 1800 psia. At that pressure the liquid began to disappear, slowly at first and then more rapidly as the upper dew point was approached. The upper dew point

for the 140°F isotherm was estimated to be 2425 psia. This pressure is believed accurate to within  $\pm 10$  psia based on visual observation. Reducing the pressure resulted in liquid "raining" out as retrograde condensation took place. The liquid took on a pale yellow hue as the retrograde region was approached. The isotherm at 110°F began to exhibit retrograde behavior at about 2200 psia. The upper dew point for this mixture was estimated to be 2495 psia. As the upper dew point was approached the fluid very suddenly became opaque indicating the isotherm to be very close to the critical temperature of that particular mixture.

### C. Comparison of Experimental Equilibrium Ratios with Predicted Values

#### (1) NGPSA Data Book

The experimental K-values of this work were compared to K-values obtained from the NGPSA data book (27). The system convergence pressure was found by extending the experimental K-values to the pressure at which the equilibrium ratio was equal to one. For the system at 110°F the convergence pressure was found to be 2620 psia and for the system at 140°F the convergence pressure was found to be 2700 psia. K-values for methane, ethane and normal hexane were taken from the NGPSA data book (27) for 4000 and 10000 psia convergence pressures for the appropriate temperatures. A linear extrapolation was made to the convergence pressure of the system. Since the K-values for carbon dioxide are only reported for a convergence pressure of 4000 psia in the NGPSA data book, additional K-values at another convergence pressure had to be found. K-value charts similar to those found in the NGPSA data book were prepared using the Winn Nomograph given by Hadden and Grayson (28). K-values for carbon dioxide were taken from these charts for a convergence pressure of 3000 psia and from the NGPSA data book for a convergence pressure of 4000 psia. Again a linear

extrapolation was made to the convergence pressure of the system. The results are shown in Figures 7 and 9 and tabulated in Tables 6 and 7 of Appendix C at 110° and 140°F respectively. The average percent deviations of the predicted K-values from the experimental K-values for each component are given in Tables 1 and 2 for the 110°F and 140°F isotherms respectively. More detailed percent deviations are given in Tables 8 and 9 in Appendix C.

## (2) BWR Equation of State

The Benedict-Webb-Rubin (BWR) equation of state has recently been the subject of considerable investigation by Bishnoi and Robinson. They have developed a new set of mixing rules (29) containing a binary interaction parameter which is readily obtainable from the experimental values of the second virial cross-coefficients. An equation for calculating the fugacity of any component in a solution was derived by Bishnoi and Robinson (31) using the BWR equation of state and the new mixing rules. A computer program based on this fugacity equation was obtained from Bishnoi (32) to predict the K-values of the multicomponent system of this study. The pure component BWR parameters for methane, carbon dioxide and ethane were obtained from the paper by Bishnoi and Robinson (30). Their technique of determining pure component BWR parameters was described in an earlier paper (29). The original BWR parameters published by Benedict, Webb and Rubin (33) were used for normal hexane. The binary interaction parameters were taken from Prausnitz and Chueh (34). The resulting predictions at 110° and 140°F are shown in Figures 7 and 9 and tabulated in Tables 6 and 7 of Appendix C respectively. The average percent deviations of the predicted K-values from the experimental K-values for each component are given in Tables 1 and 2 for the 110° and 140°F isotherms respectively. More detailed percent deviations are given in Tables 8 and 9 in Appendix C.

Methane, carbon dioxide and ethane K-values were predicted fairly well. Predicted normal hexane K-values deviated greatly from experimental K-values. The large deviations are probably due to the BWR parameters used for normal hexane. Bishnoi and Robinson (29) have dealt with the merits of their technique of determining pure component BWR parameters.

Both the Chao-Seader and Chueh-Prausnitz methods of predicting K-values for multicomponent hydrocarbon mixtures are semi-empirical, being based on thermodynamic principles and using experimental data for the evaluation of parameters. A concise comparison of these two methods was made by Besserer (35).

### (3) Chao-Seader Correlation

The Chao-Seader (CHSD) method (36, 37, 38, 39) was used to predict the K-values of this study. The results are shown in Figures 8 and 10 and tabulated in Tables 6 and 7 in Appendix C for the 110° and 140°F isotherms respectively. The average percent deviations of the predicted K-values from the experimental K-values for each component are given in Tables 1 and 2 for the 110° and 140°F isotherms respectively. More detailed percent deviations are given in Tables 8 and 9 in Appendix C. Methane and ethane K-values are predicted fairly well. Predicted carbon dioxide and normal hexane K-values deviate greatly from experimental K-values.

### (4) Chueh-Prausnitz Correlation

The experimental K-values were compared to the K-values predicted by the Chueh-Prausnitz (CHPR) method (34). The results are shown in Figures 8 and 10 and tabulated in Tables 6 and 7 in Appendix C for the 110° and 140°F isotherms respectively. Tables 1 and 2 give the average percent deviations of the predicted K-values from the experimental K-values for

each component for the 110° and 140°F isotherms respectively. More detailed percent deviations are given in Tables 8 and 9 in Appendix C. Methane and ethane K-values are predicted well. Predicted carbon dioxide and normal hexane K-values deviate greatly from experimental K-values. The large deviations are probably due to the carbon dioxide-normal hexane binary data used to evaluate the parameters. However, not enough is known about the effect of carbon dioxide on the K-values of heavy components in hydrocarbon systems.

The Chueh-Prausnitz correlation predicted the K-values of normal hexane fairly well in the region above a pressure of 1500 psia. The average percent deviation in that region was 14.4 for the 110°F isotherm and 21.2 for the 140°F isotherm. The typical behavior of the Chueh-Prausnitz correlation near the convergence pressure of a mixture is clearly shown in Figure 10.

TABLE 1  
 AVERAGE PERCENT DEVIATIONS BETWEEN EXPERIMENTAL AND PREDICTED K-VALUES  
 AT 110°F

METHOD	AVERAGE PERCENT DEVIATION			
	CH <sub>4</sub>	CO <sub>2</sub>	C <sub>2</sub> H <sub>6</sub>	C <sub>6</sub> H <sub>14</sub>
CHPR	6.5	37.7	8.8	35.6
CHSD	12.7	32.9	19.2	51.0
BWR	13.3	7.4	9.9	69.0
NGPSA	14.2	19.3	9.0	48.9

TABLE 2  
 AVERAGE PERCENT DEVIATIONS BETWEEN EXPERIMENTAL AND PREDICTED K-VALUES  
 AT 140°F

METHOD	AVERAGE PERCENT DEVIATION			
	CH <sub>4</sub>	CO <sub>2</sub>	C <sub>2</sub> H <sub>6</sub>	C <sub>6</sub> H <sub>14</sub>
CHPR	3.6	31.0	4.5	29.9
CHSD	10.2	29.0	15.6	38.9
BWR	11.4	11.3	5.9	56.7
NGPSA	14.0	15.0	2.1	38.9

## VII. CONCLUSIONS

1. A high pressure cell for the study of vapor-liquid equilibrium was built and shown to be useful by experiments on the methane-normal hexane system at 77°F.
2. Experimental K-values obtained for two mixtures of the system methane-carbon dioxide-ethane-normal hexane above the critical temperature of each mixture were compared with predicted K-values obtained from the NGPSA data book, the BWR equation of state, the Chao-Seader correlation and the Chueh-Prausnitz correlation. Methane and ethane K-values were predicted fairly well by each method. The NGPSA data book and the BWR equation of state gave reasonable K-values for carbon dioxide. Experimental normal hexane K-values were much higher than the predicted K-values of the four methods.
3. More vapor-liquid equilibria data for multicomponent hydrocarbon systems containing carbon dioxide are required to properly evaluate the effect of carbon dioxide on the K-values of such systems.



REFERENCES

1. Kuenen, J.P., Commun. Phys. Lab. Univ. Leiden, No. 4 (1892).
2. Katz, D.L. and Kurata, F., Ind. and Eng. Chem., 32, (6), 817 (1940).
3. Yarborough, L. and Vogel, J.L., Chemical Eng. Progress Symposium Series, 63, (81), 1 (1967).
4. Donnelly, H.G. and Katz, D.L., Ind. and Eng. Chem., 46, (3), 511 (1954).
5. Neumann, A. and Walch, W., Chemie-Ing.-Techn., 40, 241 (1968).
6. Kaminishi, G.I., Arai, Y., Saito, S. and Maeda, S., J. Chem. Eng. Japan, 1, 109 (1968).
7. Davis, J.A., Rodewald, N. and Kurata, F., A.I.Ch.E. Journal, 8, (4), 537 (1962).
8. Sterner, C.J., Advances in Cryogenic Engineering, 6, 467 (1961).
9. Ruhemann, M., Proc. Roy. Soc., A171, 121 (1939).
10. Ellington, R.T., Eakin, B.E., Parent, J.D., Gami, D.C. and Bloomer, O.T., "Thermodynamic and Transport Properties of Gases, Liquids and Solids", McGraw Hill, New York, 1959.
11. Price, A.R. and Kobayashi, R., J. Chem. Eng. Data, 4, 40 (1959).
- 11a. Wichterle, I. and Kobayashi, R., J. Chem. Eng. Data, 17, 9 (1972).
12. Frolich, P.K., Tauch, E.J., Hogan, J.J. and Peer, A.A., Ind. and Eng. Chem., 23, 548 (1931).
13. Hill, E.S. and Lacey, W.N., Ind. and Eng. Chem., 26, (12), 1324 (1934).
14. Sage, B.H., Webster, D.C. and Lacey, W.N., Ind. and Eng. Chem., 28, (9), 1045 (1936).
15. Boomer, C.H. and Johnson, C.A., Can. J. of Res., 16, 328 (1938).
16. Schoch, E.P., Hoffmann, A.E. and Mayfield, F.D., Ind. and Eng. Chem., 33, 688 (1941).
17. Stepanova, G.S. and Vybornova, Ya.I., Tr. Vses. Nauchn.-Issled. Inst. Prirodn. Gazov. (17-25), 203-8 (1962).
18. Shim, J. and Kohn, J.P., J. Chem. Eng. Data., 7, 3 (1962).
19. Poston, R.S. and McKetta, J.J., J. Chem. Eng. Data, 11, (3), 362 (1966).

20. Khazanova, N.E., Lesnevskaya, L.S. and Zakharova, A.V., Zh. Fiz. Khim, 41 (9), 2373 (1967).
21. Gupta, B.N., M.Sc. Thesis, Department of Chemical and Petroleum Engineering, University of Alberta, Edmonton, Alberta, 1968.
22. Friesen, R.D. and Robinson, D.B., unpublished work, University of Alberta, Edmonton, Alberta.
23. Zais, E.J. and Silberberg, I.H., J. Chem. Eng. Data, 15, 2 (1970).
24. Vairogs, J., Klekers, A.J. and Edmister, W.C., A.I.Ch.E. J., 17, (2), 308 (1971).
25. Gonzalez, M.H. and Lee, A.L., J. Chem. Eng. Data, 13, (2), 172 (1968).
26. Messner, A.E., Rosie, D.M. and Argabright, P.A., Anal. Chem., 31, 230 (1959).
27. Natural Gas Processors Suppliers Association, "Engineering Data Book", 1966.
28. Hadden, S.T., and Grayson, H.G., Hydrocarbon Processing and Petroleum Refiner, 40, (9), 207 (1961).
29. Bishnoi, P.R. and Robinson, D.B., Can. J. of Chem. Eng., 49, 642 (1971).
30. Bishnoi, P.R. and Robinson, D.B., Can. J. of Chem. Eng., 50, 101 (1972).
31. Bishnoi, P.R. and Robinson, D.B., Can. J. of Chem. Eng., 50, 506 (1972).
32. Bishnoi, P.R., private communication.
33. Benedict, M., Webb, G.B. and Rubin, L.C., Chem. Eng. Prog., 47, 419 (1951).
34. Prausnitz, J.M. and Chueh, P.L., "Computer Calculations for High-Pressure Vapor-Liquid Equilibria", Prentice-Hall, Inc., N.J., 1968.
35. Besserer, G.R.J., Ph.D. Thesis, Department of Chemical and Petroleum Engineering, University of Alberta, Edmonton, Alberta, 1972.
36. Prausnitz, J.M., Edmister, W.C. and Chao, K.C., A.I.Ch.E. J., 6, 214 (1960).
37. Chao, K.C. and Seader, J.D., A.I.Ch.E. J., 7, 598 (1961).
38. Cavett, R.H., American Petroleum Institute, Division of Refining, 42, 351 (1962).
39. Erbar, J.H., NGPA K and H Program (1962).

APPENDICES

APPENDIX A  
CHARGING PROCEDURE

The following procedure was used to charge the cell.

1. Drive the pistons to their extreme ends to maximize the cell volume.
2. Evacuate the cell and circulation system.
3. Connect the graduated liquid charging reservoir to the cell.
4. Introduce approximately 15 cc of normal hexane to the reservoir.
5. Bubble methane through the normal hexane.
6. Allow 5 cc of normal hexane to be drawn into the cell.
7. Allow the charge gas to flow into the cell and circulation system until a pressure of about 220 psia is achieved.
8. Start the circulation system.
9. Increase the pressure in the system until a single phase is achieved by moving the pistons toward one another using the double-acting mercury pump.
10. Allow the circulation system to operate for about 3 hours or until samples taken from the top and bottom of the cell are in agreement.

APPENDIX B  
SAMPLING PROCEDURE

The following procedure was used to take samples from the cell.

(a) Vapor Sampling

1. Evacuate the vapor sampling system.
2. Isolate the cavity in the vapor sampling valve by closing the valve.
3. Circulate vapor for about 30 minutes to clear the lines of liquid.
4. Open the vapor sampling valve to allow a sample to enter the cavity and then close the valve.
5. Isolate the vapor sampling system from the cell.
6. Remove the vapor sampling valve from the vapor sampling system and connect it to the injection system of the gas chromatograph.
7. Analyze the vapor sample.
8. Return the vapor sampling valve to the vapor sample system.

(b) Liquid Sampling

1. Isolate and evacuate the liquid sampling system.
2. Isolate the cavity of the liquid sampling valve.
3. Isolate the bottom of the circulation pump from the cell.
4. Shut the circulation pump off.
5. Allow about 30 minutes for the liquid in the cell to drain down to the vicinity of the liquid sampling valve. During this time run the contents of the cell up and down several times with the displacement pump.
6. Allow the liquid to be drawn into the liquid sampling system through the valve nearest the cell.
7. Open the liquid sampling valve to allow a sample into the cavity and then close it.
8. Open the other valve of the liquid sampling system and pump vapor through the liquid sampling system for about 15 minutes.
9. Isolate the liquid sampling system.

10. Remove the liquid sampling valve from the liquid sampling system and connect it to the injection system of the gas chromatograph.
11. Analyze the liquid sample.
12. Return the liquid sampling valve to the liquid sampling system.

APPENDIX C  
TABULATED DATA

TABLE 3

VAPOR-LIQUID EQUILIBRIUM DATA FOR THE SYSTEM  
METHANE-NORMAL HEXANE AT 77°F

PRESSURE atm.	MOLE FRACTION METHANE	
	Vapor	Liquid
9.4		0.0498 0.0464
9.5	0.9532 0.9512	
19.4	0.9801 0.9773	0.0984 0.1057
29.2		0.1454 0.1399
29.4	0.9820 0.9779	
39.2		0.2036 0.2040
39.4	0.9817 0.9820	
49.4	0.9842 0.9820	
49.7		0.2460 0.2446
59.4		0.2722 0.2747
59.4	0.9848 0.9862	
69.4	0.9857 0.9884	
69.8		0.3140 0.2888
79.4	0.9840 0.9857	



TABLE 3 (continued)

PRESSURE atm.	MOLE FRACTION METHANE	
	Vapor	Liquid
79.5		0.3248
		0.3479
89.4	0.9873	
	0.9868	
89.7		0.3814
		0.3899
99.4		0.4160
		0.4218
99.4	0.9860	
	0.9869	
119.6		0.4948
		0.4812

TABLE 4  
COMPARISON OF METHANE-NORMAL HEXANE LIQUID PHASE DATA  
WITH THAT OF SHIM AND KOHN (18)  
TEMPERATURE = 77°F

PRESSURE atm.	MOLE FRACTION METHANE		DIFFERENCE*
	Shim and Kohn	This Work	
10	0.0490	0.0508	0.0018
20	0.0978	0.1070	0.0092
30	0.1450	0.1530	0.0080
40	0.1890	0.1975	0.0085
50	0.2316	0.2380	0.0062
60	0.2710	0.2770	0.0060
70	0.3090	0.3150	0.0060
80	0.3447	0.3520	0.0073
90	0.3810	0.3870	0.0060
100	0.4125	0.4210	0.0085
120	0.4740	0.4880	0.0140

\* Difference denotes This Work minus that of Shim and Kohn.

TABLE 5  
COMPARISON OF METHANE-NORMAL HEXANE VAPOR PHASE DATA  
WITH THAT OF SHIM AND KOHN (18)  
TEMPERATURE = 77°F

PRESSURE atm.	MOLE FRACTION METHANE		DIFFERENCE*
	Shim and Kohn	This Work	
10	0.9530	0.9535	0.0005
20	0.9728	0.9738	0.0010
30	0.9795	0.9803	0.0008
40	0.9830	0.9826	-0.0004
50	0.9850	0.9841	-0.0009
60	0.9863	0.9852	-0.0011
70	0.9871	0.9860	-0.0011
80	0.9868	0.9861	-0.0007
90	0.9854	0.9860	0.0006
100	0.9833	0.9853	0.0020

\* Difference denotes This Work minus that of Shim and Kohn.

TABLE 6  
 EXPERIMENTAL AND PREDICTED EQUILIBRIUM RATIOS FOR THE  
 METHANE-CARBON DIOXIDE-ETHANE-NORMAL HEXANE SYSTEM  
 AT 110°F

PRESSURE psia	COMPONENT	SMOOTHED EXP'L	EQUILIBRIUM RATIO			
			CHPR	CHSD	BWR	NGPSA P <sub>cv</sub> = 2620
300	CH <sub>4</sub>	10.45	10.43	9.52	9.04	10.29
	CO <sub>2</sub>	6.60	3.88	3.90	6.12	4.99
	C <sub>2</sub> H <sub>6</sub>	2.33	2.42	2.10	2.14	2.12
	C <sub>6</sub> H <sub>14</sub>	0.103	0.035	0.035	0.028	0.039
500	CH <sub>4</sub>	7.55	6.35	5.92	6.07	6.51
	CO <sub>2</sub>	3.99	2.45	2.37	4.26	3.11
	C <sub>2</sub> H <sub>6</sub>	1.62	1.58	1.37	1.69	1.44
	C <sub>6</sub> H <sub>14</sub>	0.082	0.030	0.030	0.022	0.033
750	CH <sub>4</sub>	4.80	4.30	4.12	4.06	4.63
	CO <sub>2</sub>	2.84	1.73	1.64	2.84	2.21
	C <sub>2</sub> H <sub>6</sub>	1.29	1.17	1.02	1.10	1.10
	C <sub>6</sub> H <sub>14</sub>	0.070	0.031	0.031	0.021	0.033
1000	CH <sub>4</sub>	3.52	3.27	3.23	3.22	3.63
	CO <sub>2</sub>	2.27	1.38	1.31	2.30	1.71
	C <sub>2</sub> H <sub>6</sub>	1.04	0.978	0.855	0.944	0.948
	C <sub>6</sub> H <sub>14</sub>	0.068	0.038	0.036	0.023	0.038
1250	CH <sub>4</sub>	2.79	2.64	2.70	2.70	3.03
	CO <sub>2</sub>	1.90	1.17	1.15	1.98	1.42
	C <sub>2</sub> H <sub>6</sub>	0.940	0.873	0.769	0.864	0.878
	C <sub>6</sub> H <sub>14</sub>	0.074	0.049	0.044	0.027	0.046
1500	CH <sub>4</sub>	2.31	2.20	2.34	2.36	2.63
	CO <sub>2</sub>	1.66	1.03	1.07	1.77	1.29
	C <sub>2</sub> H <sub>6</sub>	0.890	0.813	0.722	0.821	0.838
	C <sub>6</sub> H <sub>14</sub>	0.089	0.069	0.056	0.032	0.057

TABLE 6 (continued)

PRESSURE	COMPONENT	EQUILIBRIUM RATIO				
		SMOOTHED EXP'L	CHPR	CHSD	BWR	NGPSA $P_{cv} = 2620$
1750	CH <sub>4</sub>	1.92	1.88	2.09	2.10	2.33
	CO <sub>2</sub>	1.48	0.935	1.05	1.63	1.24
	C <sub>2</sub> H <sub>6</sub>	0.890	0.782	0.098	0.801	0.829
	C <sub>6</sub> H <sub>14</sub>	0.118	0.102	0.071	0.041	0.070
2000	CH <sub>4</sub>	1.61	1.64	1.90	1.91	2.04
	CO <sub>2</sub>	1.34	0.867	1.08	1.52	1.20
	C <sub>2</sub> H <sub>6</sub>	0.910	0.775	0.689	0.796	0.832
	C <sub>6</sub> H <sub>14</sub>	0.173	0.159	0.089	0.052	0.090
2250	CH <sub>4</sub>	1.35	1.49	1.76	1.75	1.83
	CO <sub>2</sub>	1.23	0.827	1.15	1.44	1.15
	C <sub>2</sub> H <sub>6</sub>	0.930	0.789	0.686	0.800	0.845
	C <sub>6</sub> H <sub>14</sub>	0.280	0.243	0.109	0.067	0.116

TABLE 7  
 EXPERIMENTAL AND PREDICTED EQUILIBRIUM RATIOS FOR THE  
 METHANE-CARBON DIOXIDE-ETHANE-NORMAL HEXANE SYSTEM  
 AT 140°F

PRESSURE psia	COMPONENT	EQUILIBRIUM RATIO				
		SMOOTHED EXP'L	CHPR	CHSD	BWR	NGPSA P <sub>cv</sub> = 2700
300	CH <sub>4</sub>	11.70	11.01	10.19	9.64	10.77
	CO <sub>2</sub>	7.35	4.71	4.78	6.68	5.86
	C <sub>2</sub> H <sub>6</sub>	2.62	2.91	2.56	2.54	2.62
	C <sub>6</sub> H <sub>14</sub>	0.118	0.059	0.059	0.051	0.065
500	CH <sub>4</sub>	7.01	6.70	6.32	6.07	6.69
	CO <sub>2</sub>	4.61	2.95	2.86	4.26	3.85
	C <sub>2</sub> H <sub>6</sub>	1.83	1.89	1.64	1.69	1.73
	C <sub>6</sub> H <sub>14</sub>	0.084	0.048	0.049	0.039	0.051
750	CH <sub>4</sub>	4.71	4.53	4.38	4.27	4.75
	CO <sub>2</sub>	3.21	2.07	1.95	3.05	2.60
	C <sub>2</sub> H <sub>6</sub>	1.38	1.38	1.18	1.27	1.32
	C <sub>6</sub> H <sub>14</sub>	0.071	0.048	0.048	0.036	0.047
1000	CH <sub>4</sub>	3.56	3.43	3.41	3.36	3.71
	CO <sub>2</sub>	2.52	1.63	1.53	2.45	1.97
	C <sub>2</sub> H <sub>6</sub>	1.13	1.14	0.967	1.08	1.12
	C <sub>6</sub> H <sub>14</sub>	0.075	0.055	0.053	0.037	0.051
1250	CH <sub>4</sub>	2.80	2.75	2.83	2.81	3.14
	CO <sub>2</sub>	2.00	1.37	1.32	2.10	1.63
	C <sub>2</sub> H <sub>6</sub>	1.01	1.00	0.845	0.969	1.02
	C <sub>6</sub> H <sub>14</sub>	0.088	0.067	0.062	0.041	0.060
1500	CH <sub>4</sub>	2.27	2.29	2.44	2.44	2.71
	CO <sub>2</sub>	1.65	1.19	1.21	1.86	1.43
	C <sub>2</sub> H <sub>6</sub>	0.955	0.921	0.772	0.907	0.965
	C <sub>6</sub> H <sub>14</sub>	0.112	0.089	0.074	0.048	0.072

TABLE 7 (continued)

PRESSURE	COMPONENT	EQUILIBRIUM RATIO				
		SMOOTHED EXP'L	CHPR	CHSD	BWR	NGPSA $P_{cv} = 2700$
1750	CH <sub>4</sub>	1.89	1.94	2.17	2.16	2.41
	CO <sub>2</sub>	1.41	1.06	1.17	1.69	1.35
	C <sub>2</sub> H <sub>6</sub>	0.932	0.870	0.727	0.872	0.923
	C <sub>6</sub> H <sub>14</sub>	0.150	0.123	0.090	0.057	0.090
2000	CH <sub>4</sub>	1.58	1.67	1.96	1.95	2.14
	CO <sub>2</sub>	1.22	0.959	1.19	1.57	1.30
	C <sub>2</sub> H <sub>6</sub>	0.935	0.843	0.698	0.854	0.906
	C <sub>6</sub> H <sub>14</sub>	0.239	0.179	0.109	0.070	0.111

TABLE 7 (continued)

PRESSURE	COMPONENT	EQUILIBRIUM RATIO				
		SMOOTHED EXP'L	CHPR	CHSD	BWR	NGPSA P <sub>cv</sub> = 2700
1750	CH <sub>4</sub>	1.89	1.94	2.17	2.16	2.41
	CO <sub>2</sub>	1.41	1.06	1.17	1.69	1.35
	C <sub>2</sub> H <sub>6</sub>	0.932	0.870	0.727	0.872	0.923
	C <sub>6</sub> H <sub>14</sub>	0.150	0.123	0.090	0.057	0.090
2000	CH <sub>4</sub>	1.58	1.67	1.96	1.95	2.14
	CO <sub>2</sub>	1.22	0.959	1.19	1.57	1.30
	C <sub>2</sub> H <sub>6</sub>	0.935	0.843	0.698	0.854	0.906
	C <sub>6</sub> H <sub>14</sub>	0.239	0.179	0.109	0.070	0.111



TABLE 9  
 PERCENT DEVIATIONS BETWEEN EXPERIMENTAL AND PREDICTED K-VALUES  
 AT 140°F

COMPONENT	PRESSURE psia	PERCENT DEVIATION			
		CHPR	CHSD	BWR	NGPSA
CH <sub>4</sub>	300	5.9	12.9	17.6	7.9
	500	4.4	9.8	13.4	4.6
	750	3.8	7.0	9.3	- 0.8
	1000	3.7	4.2	5.6	- 4.2
	1250	1.8	- 1.1	- 0.4	-12.1
	1500	- 0.9	- 7.5	- 7.5	-19.4
	1750	- 2.6	-14.8	-14.3	-27.5
	2000	- 5.7	-24.1	-23.4	-35.4
CO <sub>2</sub>	300	35.9	35.0	9.1	20.3
	500	36.0	38.0	7.6	16.5
	750	35.5	39.3	5.0	19.0
	1000	35.3	39.3	2.8	21.8
	1250	31.5	34.0	- 5.0	18.5
	1500	27.9	26.7	-12.7	13.3
	1750	24.8	17.0	-19.9	4.3
	2000	21.4	2.5	-28.7	- 6.6
C <sub>2</sub> H <sub>6</sub>	300	-11.1	2.3	3.1	0.0
	500	- 3.3	10.4	7.7	5.5
	750	0.0	14.5	8.0	4.3
	1000	- 0.9	14.4	4.4	0.9
	1250	1.0	16.3	4.1	- 1.0
	1500	3.6	19.2	5.0	- 1.0
	1750	6.7	22.0	6.4	1.0
	2000	9.8	25.3	8.7	3.1
C <sub>6</sub> H <sub>14</sub>	300	50.0	50.0	56.8	44.9
	500	42.9	41.7	53.6	39.3
	750	32.4	32.4	49.3	33.8
	1000	26.7	29.3	50.7	32.0
	1250	23.9	29.5	53.4	31.8
	1500	20.5	33.9	57.1	35.7
	1750	18.0	40.0	62.0	40.0
	2000	25.1	54.4	70.7	53.6

TABLE 10  
 VAPOR-LIQUID EQUILIBRIUM DATA FOR THE METHANE-  
 CARBON DIOXIDE-ETHANE-NORMAL HEXANE SYSTEM  
 AT 110°F

OVERALL COMPOSITION IN MOLE FRACTION

COMPONENT	TOP OF CELL	BOTTOM OF CELL
CH <sub>4</sub>	0.6998	0.6989
CO <sub>2</sub>	0.0925	0.0851
C <sub>2</sub> H <sub>6</sub>	0.0759	0.0751
C <sub>6</sub> H <sub>14</sub>	0.1315	0.1407

PRESSURE psia	COMPONENT	MOLE FRACTION	
		Vapor	Liquid
300	CH <sub>4</sub>	0.7393	0.0707
	CO <sub>2</sub>	0.1069	0.0161
	C <sub>2</sub> H <sub>6</sub>	0.0680	0.0289
	C <sub>6</sub> H <sub>14</sub>	0.0857	0.8841
500	CH <sub>4</sub>	0.7404	0.1040
	CO <sub>2</sub>	0.1049	0.0262
	C <sub>2</sub> H <sub>6</sub>	0.0634	0.0390
	C <sub>6</sub> H <sub>14</sub>	0.0911	0.8306
765	CH <sub>4</sub>	0.7805	0.1645
	CO <sub>2</sub>	0.1058	0.0336
	C <sub>2</sub> H <sub>6</sub>	0.0654	0.0528
	C <sub>6</sub> H <sub>14</sub>	0.0481	0.7489
765	CH <sub>4</sub>	0.7858	
	CO <sub>2</sub>	0.0917	
	C <sub>2</sub> H <sub>6</sub>	0.0661	
	C <sub>6</sub> H <sub>14</sub>	0.0562	

TABLE 10 (continued)

PRESSURE psia	COMPONENT	MOLE FRACTION	
		Vapor	Liquid
1000	CH <sub>4</sub>	0.7590	0.2120
	CO <sub>2</sub>	0.0908	0.0440
	C <sub>2</sub> H <sub>6</sub>	0.0677	0.0653
	C <sub>6</sub> H <sub>14</sub>	0.0822	0.6785
1000	CH <sub>4</sub>	0.7817	
	CO <sub>2</sub>	0.1013	
	C <sub>2</sub> H <sub>6</sub>	0.0675	
	C <sub>6</sub> H <sub>14</sub>	0.0493	
1250	CH <sub>4</sub>	0.7876	0.2711
	CO <sub>2</sub>	0.1096	0.0520
	C <sub>2</sub> H <sub>6</sub>	0.0581	0.0684
	C <sub>6</sub> H <sub>14</sub>	0.0445	0.6082
1250	CH <sub>4</sub>	0.7874	
	CO <sub>2</sub>	0.0953	
	C <sub>2</sub> H <sub>6</sub>	0.0690	
	C <sub>6</sub> H <sub>14</sub>	0.0481	
1500	CH <sub>4</sub>	0.7567	0.3812
	CO <sub>2</sub>	0.1183	0.0663
	C <sub>2</sub> H <sub>6</sub>	0.0766	0.0768
	C <sub>6</sub> H <sub>14</sub>	0.0483	0.4755
1500	CH <sub>4</sub>	0.7806	
	CO <sub>2</sub>	0.1082	
	C <sub>2</sub> H <sub>6</sub>	0.0654	
	C <sub>6</sub> H <sub>14</sub>	0.0456	
1750	CH <sub>4</sub>	0.7818	0.3684
	CO <sub>2</sub>	0.1011	0.0671
	C <sub>2</sub> H <sub>6</sub>	0.0655	0.0781
	C <sub>6</sub> H <sub>14</sub>	0.0513	0.4862

TABLE 10 (continued)

PRESSURE psia	COMPONENT	MOLE FRACTION	
		Vapor	Liquid
1750	CH <sub>4</sub>	0.7750	
	CO <sub>2</sub>	0.0993	
	C <sub>2</sub> H <sub>6</sub>	0.0758	
	C <sub>6</sub> H <sub>14</sub>	0.0496	
2000	CH <sub>4</sub>	0.7726	0.5522
	CO <sub>2</sub>	0.0984	0.0787
	C <sub>2</sub> H <sub>6</sub>	0.0699	0.0745
	C <sub>6</sub> H <sub>14</sub>	0.0589	0.2944
2000	CH <sub>4</sub>	0.7655	0.4911
	CO <sub>2</sub>	0.1000	0.0732
	C <sub>2</sub> H <sub>6</sub>	0.0738	0.0871
	C <sub>6</sub> H <sub>14</sub>	0.0606	0.3484
2265	CH <sub>4</sub>	0.7432	0.5431
	CO <sub>2</sub>	0.0970	0.0786
	C <sub>2</sub> H <sub>6</sub>	0.0804	0.0818
	C <sub>6</sub> H <sub>14</sub>	0.0792	0.2963
2265	CH <sub>4</sub>	0.7067	
	CO <sub>2</sub>	0.1109	
	C <sub>2</sub> H <sub>6</sub>	0.0828	
	C <sub>6</sub> H <sub>14</sub>	0.0994	

TABLE 11  
 VAPOR-LIQUID EQUILIBRIUM DATA FOR THE METHANE-  
 CARBON DIOXIDE-ETHANE-NORMAL HEXANE SYSTEM  
 AT 140°F

OVERALL COMPOSITION IN MOLE FRACTION

PRESSURE psia	COMPONENT	MOLE FRACTION	
		Vapor	Liquid
	CH <sub>4</sub>	0.7333	0.7330
	CO <sub>2</sub>	0.0886	0.0893
	C <sub>2</sub> H <sub>6</sub>	0.0660	0.0661
	C <sub>6</sub> H <sub>14</sub>	0.1119	0.1114
265	CH <sub>4</sub>	0.7470	0.0584
	CO <sub>2</sub>	0.0947	0.0128
	C <sub>2</sub> H <sub>6</sub>	0.0683	0.0275
	C <sub>6</sub> H <sub>14</sub>	0.0898	0.9011
538	CH <sub>4</sub>	0.7559	0.1024
	CO <sub>2</sub>	0.0933	0.0213
	C <sub>2</sub> H <sub>6</sub>	0.0676	0.0415
	C <sub>6</sub> H <sub>14</sub>	0.0830	0.8346
765	CH <sub>4</sub>	0.7699	0.1635
	CO <sub>2</sub>	0.1002	0.0293
	C <sub>2</sub> H <sub>6</sub>	0.0722	0.0474
	C <sub>6</sub> H <sub>14</sub>	0.0574	0.7596
765	CH <sub>4</sub>	0.7818	
	CO <sub>2</sub>	0.0932	
	C <sub>2</sub> H <sub>6</sub>	0.0713	
	C <sub>6</sub> H <sub>14</sub>	0.0535	

TABLE 11 (continued)

PRESSURE psia	COMPONENT	MOLE FRACTION	
		Vapor	Liquid
765	CH <sub>4</sub>	0.7779	
	CO <sub>2</sub>	0.0967	
	C <sub>2</sub> H <sub>6</sub>	0.0697	
	C <sub>6</sub> H <sub>14</sub>	0.0555	
1015	CH <sub>4</sub>	0.7863	0.2453
	CO <sub>2</sub>	0.0986	0.0518
	C <sub>2</sub> H <sub>6</sub>	0.0678	0.0667
	C <sub>6</sub> H <sub>14</sub>	0.0470	0.6359
1015	CH <sub>4</sub>	0.7928	
	CO <sub>2</sub>	0.0924	
	C <sub>2</sub> H <sub>6</sub>	0.0676	
	C <sub>6</sub> H <sub>14</sub>	0.0470	
1015	CH <sub>4</sub>	0.7881	0.1971
	CO <sub>2</sub>	0.0927	0.0381
	C <sub>2</sub> H <sub>6</sub>	0.0670	0.0561
	C <sub>6</sub> H <sub>14</sub>	0.0520	0.7086
1515	CH <sub>4</sub>	0.7733	0.3364
	CO <sub>2</sub>	0.0983	0.0580
	C <sub>2</sub> H <sub>6</sub>	0.0760	0.0690
	C <sub>6</sub> H <sub>14</sub>	0.0522	0.5363
1515	CH <sub>4</sub>	0.7804	
	CO <sub>2</sub>	0.0942	
	C <sub>2</sub> H <sub>6</sub>	0.0704	
	C <sub>6</sub> H <sub>14</sub>	0.0548	
1515	CH <sub>4</sub>	0.7872	
	CO <sub>2</sub>	0.0939	
	C <sub>2</sub> H <sub>6</sub>	0.0664	
	C <sub>6</sub> H <sub>14</sub>	0.0523	

TABLE 11 (continued)

PRESSURE psia	COMPONENT	MOLE FRACTION	
		Vapor	Liquid
2004	CH <sub>4</sub>	0.7598	0.7025
	CO <sub>2</sub>	0.0943	0.0836
	C <sub>2</sub> H <sub>6</sub>	0.0667	0.0656
	C <sub>6</sub> H <sub>14</sub>	0.0791	0.1481
2004	CH <sub>4</sub>	0.7545	
	CO <sub>2</sub>	0.1048	
	C <sub>2</sub> H <sub>6</sub>	0.0657	
	C <sub>6</sub> H <sub>14</sub>	0.0748	

APPENDIX D  
EQUIPMENT EVALUATION AND RECOMMENDATIONS

1. A new valve should be developed so that in-line sampling would be possible.
2. The expansion coil in the base of the cell should be replaced with a hollow rod connected to the piston and running through a packing in the bottom of the cell.
3. Additional studies should be conducted on multicomponent hydrocarbon systems containing carbon dioxide and heavy hydrocarbons (pentanes +).



APPENDIX E  
CALIBRATIONS

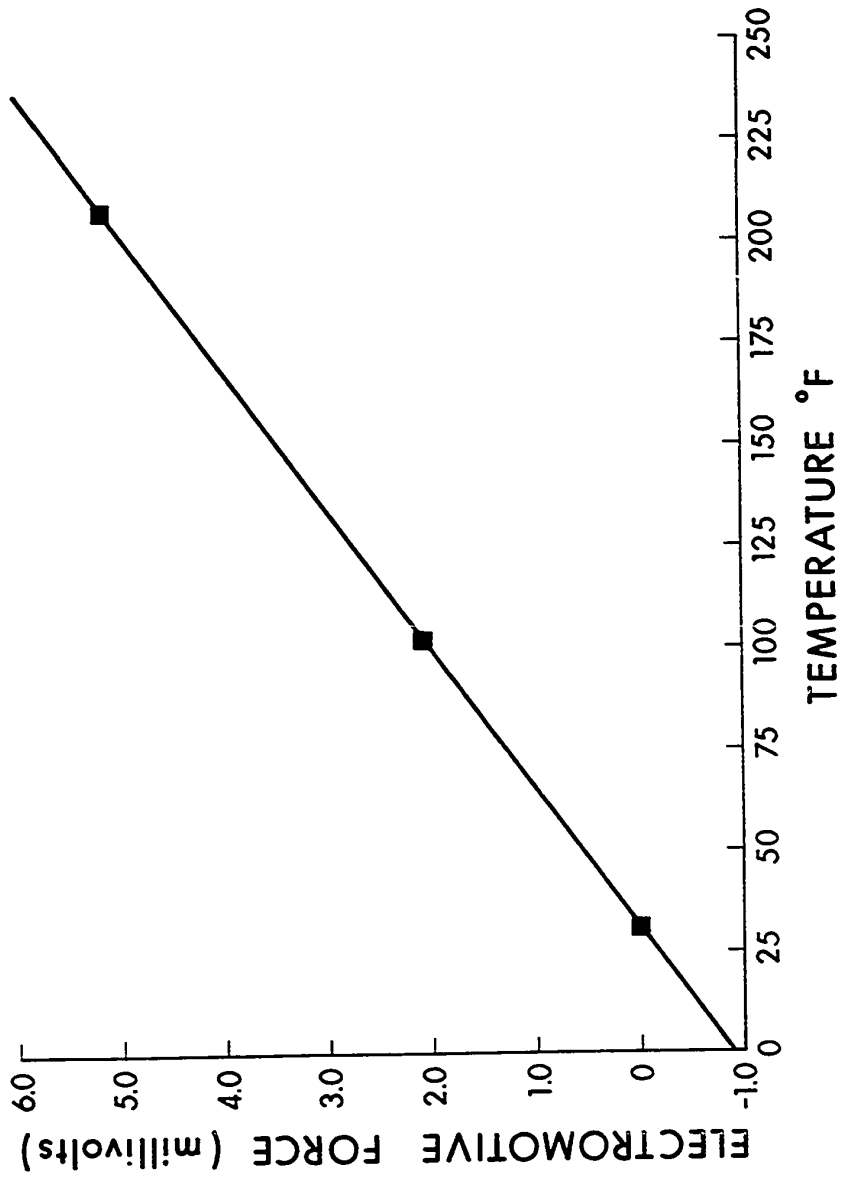


Figure 11 Thermocouple Calibration

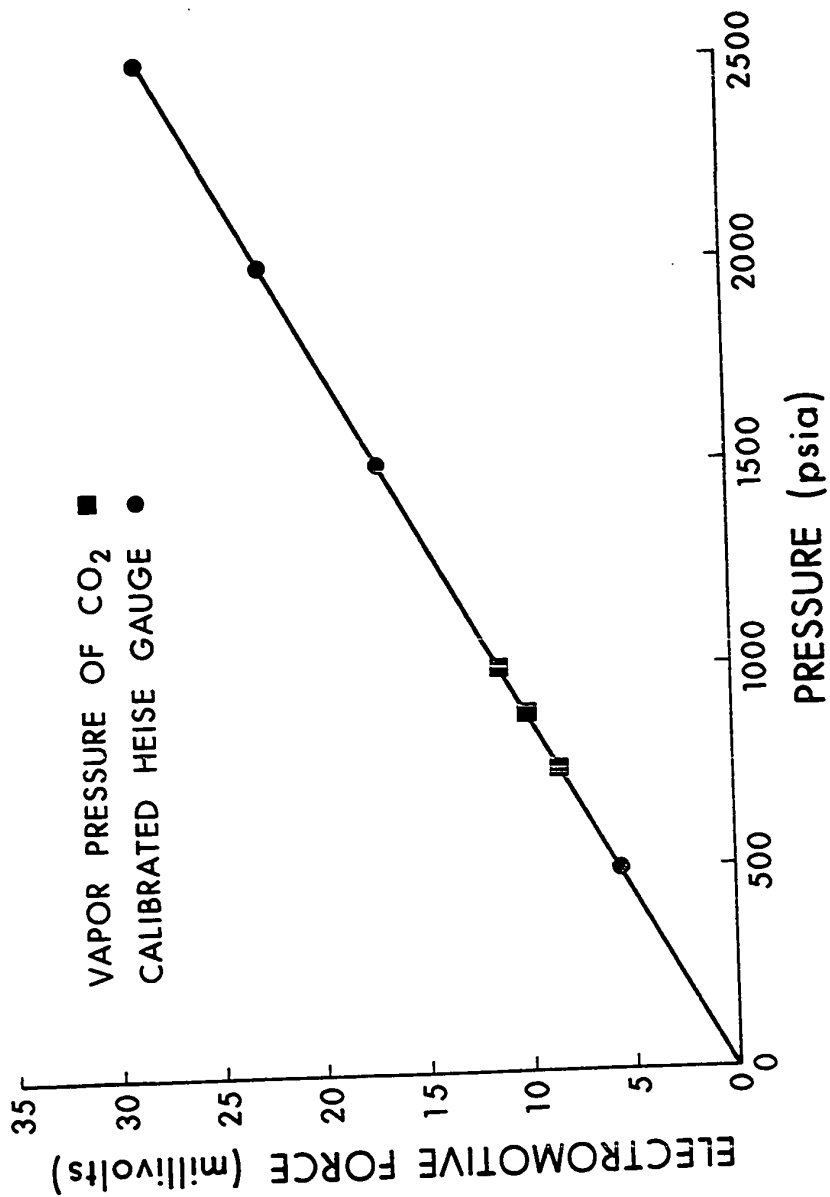


Figure 12 Transducer Calibration

APPENDIX F  
CALCULATIONS

The following equation was used to calculate the mole fraction of a component from chromatographic data.

$$Z_{CH_4} = \frac{\frac{A_{CH_4} \cdot R_{CH_4}}{E_{CH_4}}}{\frac{A_{CH_4} \cdot R_{CH_4}}{E_{CH_4}} + \frac{A_{CO_2} \cdot R_{CO_2}}{E_{CO_2}} + \frac{A_{C_2H_6} \cdot R_{C_2H_6}}{E_{C_2H_6}} + \frac{A_{C_6H_{14}} \cdot R_{C_6H_{14}}}{E_{C_6H_{14}}}}$$

where      Z = mole fraction  
            A = peak area  
            R = response factor  
            E = enhancement factor

The response factors were obtained from the paper by Messner et al. (26). The enhancement factors were taken from the graph shown in Figure 13.

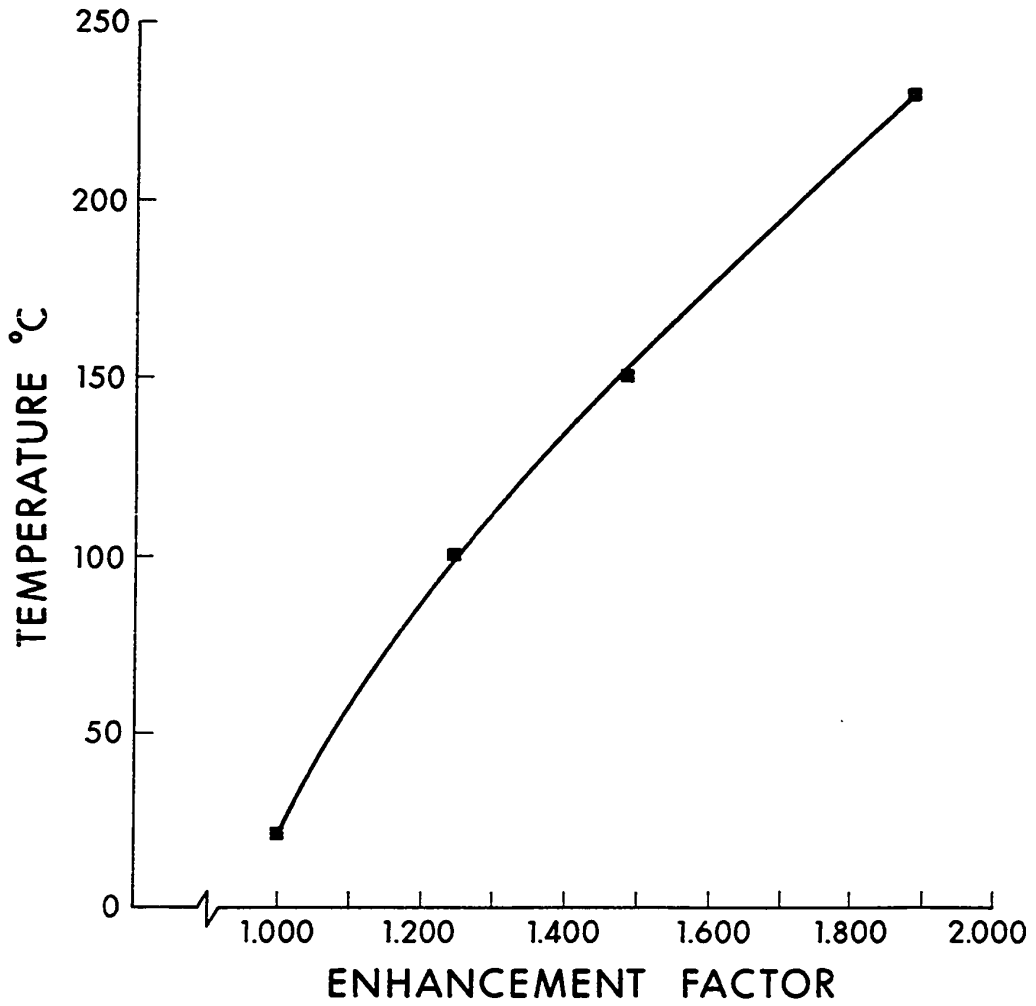


Figure 13 Gas Chromatograph Temperature-Enhancement Factor Curve